AD-A087 413 LITTON SYSTEMS INC SAN CARLOS CA ELECTRON TUBE DIV F/G 9/1
NON-PERIODIC HELIX TWT STUDY.(U)
MAY 80 N00173-76-C-0194

UNCLASSIFIED NL

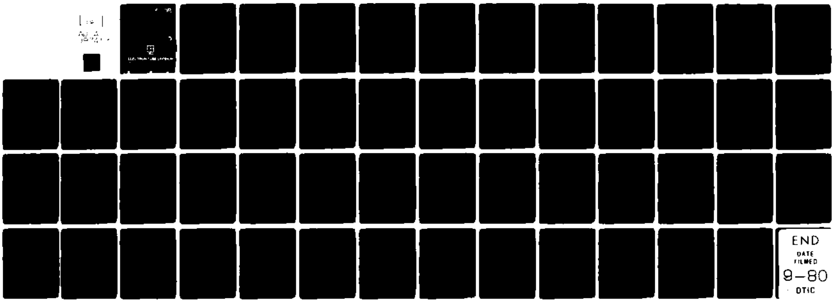

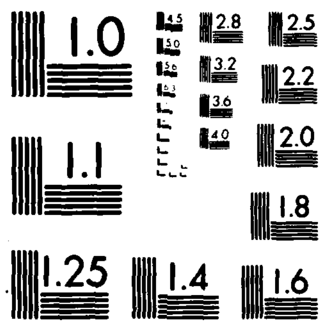


MICROCOPY RESOLUTION TEST CHART

LEVEL

ADA087413

DTIC
ELECTE
JUL 31 1980
C
D

Litton

# ELECTRON TUBE DIVISION

This document has been approved for public release and sale; its distribution is unlimited.

FILE COPY

80 6 11 040

2

# NON-PERIODIC HELIX TWT STUDY

EXTENSION OF CONTRACT

N00173-76-C-0194

FINAL REPORT

CLIN 0001AB, EXHIBIT A ITEM A005



PREPARED BY

LITTON SYSTEMS, INC.
dba LITTON INDUSTRIES
ELECTRON TUBE DIVISION
960 INDUSTRIAL ROAD
SAN CARLOS, CALIFORNIA 94070

PREPARED FOR

NAVAL RESEARCH LABORATORY
WASHINGTON, D. C. 20375

May 1980

# TABLE OF CONTENTS

## INDEX OF FIGURES

## 1.0 INTRODUCTION

The purpose of this contract was to determine the feasibility of using various techniques to increase the operating voltages and peak power levels of helix type traveling-wave tubes. → p 46

Two approaches were investigated in sequence. The first approach dealt with strapped multifilar helixes. The work done and conclusions reached in this effort are described in Report #N00173-76-C-0001.

The second approach deals with non-periodic helix loading. This is accomplished by shifting the relative position of the ceramic helix supports from turn to turn. This work, which represented a change in scope for the program, was proposed and approved in April 1978. Most of the work done on this approach was completed in March 1979. At that time, a tube was built. Subsequent testing of that vehicle revealed that it would be necessary to perform additional tests at higher voltages than anticipated. This required the use of equipment and personnel not normally available to the group conducting the investigation. This testing was not

## 1.0 INTRODUCTION (continued)

accomplished. The limited testing that was done was performed at the expense of Litton Industries, but the results are described in this report, as they are germane to the investigation. A description of all work done and conclusions drawn from the study of non-periodic helix loading is contained in Section 2 of this report.

In Section 3, the results of the work described in Section 2 are summarized. Proposed studies derived from our analysis of the results are described in Section 4.

## 2.0 TECHNICAL DISCUSSION

### 2.1 Introduction and Stopband Requirements

The purpose of this study is to develop a helix type circuit which suppresses oscillations at higher voltages than have previously been possible, with potential application at I-J band.

Because the helix is a periodic structure, Floquet's Theorem applies and all the space harmonics must be present to match the boundary conditions of the structure. The propagation constant for the nth harmonic is given by

$$\beta_n = \beta_o + \frac{2\pi n}{p}$$

The principal space harmonics of concern in the TWT are n = 0 and n = -1. They are respectively the fundamental forward wave and the backward wave space harmonics.

Figure 1 is a Brillouin diagram of a basic helix circuit, showing the fundamental forward and backward wave modes, and the point at which BWO may occur. From this, the following observations can be made:

1. The backward wave mode is a mirror image of the forward wave mode, about $\beta p = 0$.

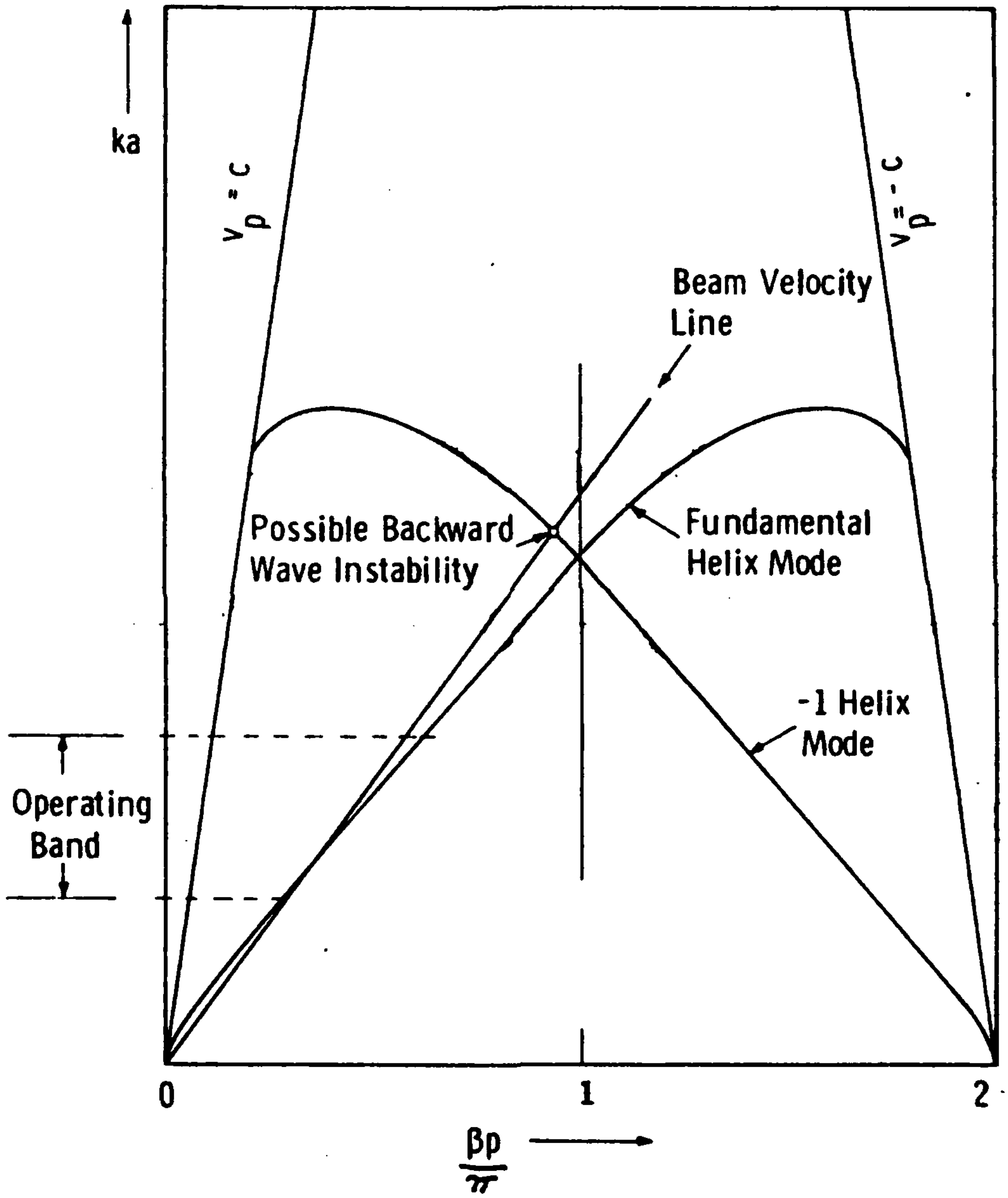


BASIC HELIX CIRCUIT

FIGURE 1

2.1 Introduction and Stopband Requirements (continued)

2. Slight changes in the slope of the mode line can cause substantial changes in the backward wave frequency.

3. Forward wave interaction occurs over a broad band while backward wave interaction occurs at a single frequency.

On the basis of this type of analysis, several techniques for BWO suppression have been proposed. Two such techniques will be discussed here.

The first technique takes advantage of the narrow bandwidth of the BWO at a given beam voltage and helix pitch. By tapering the pitch, the normalized mode slope changes and the BWO frequency shifts. In the proposal made in April on this program, this type of oscillation suppression was proposed with the change in loading resulting from a shift in wedge spacing causing the change in circuit velocity otherwise brought about by changing the pitch. This technique works best in cases where the stability is marginal.

2.1 Introduction and Stopband Requirements (continued)

The second technique includes the introduction of stopband in both the forward and backward wave modes which occurs at the BWO interaction frequency. If the wedge support pattern repeats at less than the helix pitch, a stopband should occur in the forward wave mode at the point where

$$\left(\frac{\beta p}{\pi}\right)_f = \frac{\text{helix pitch}}{\text{wedge pattern period}}$$

If the symmetry found in the basic circuit is maintained, a stopband should occur in the backward wave mode at the point where

$$\left(\frac{\beta p}{\pi}\right)_b = 2 - \left(\frac{\beta p}{\pi}\right)_f$$

In the principal circuit investigated, the wedge pattern period is 5/6 of the pitch. Therefore, the forward wave stopband occurs at $\left(\frac{\beta p}{\pi}\right)_f = 1.2$ and the backward wave stopband occurs at $\left(\frac{\beta p}{\pi}\right)_b = 0.8$. An isometric view of the circuit is shown in Figure 2. The amount of rotation of wedges from one turn to the next is $60^\circ$. An isometric view of the unwound helix tape with dielectric wedges attached is shown in Figure 3. Note that a full wedge period is 5/6 of a turn on the helix. If this technique works as predicted, it should suppress BWO even in cases where an ordinary circuit would be operating well into

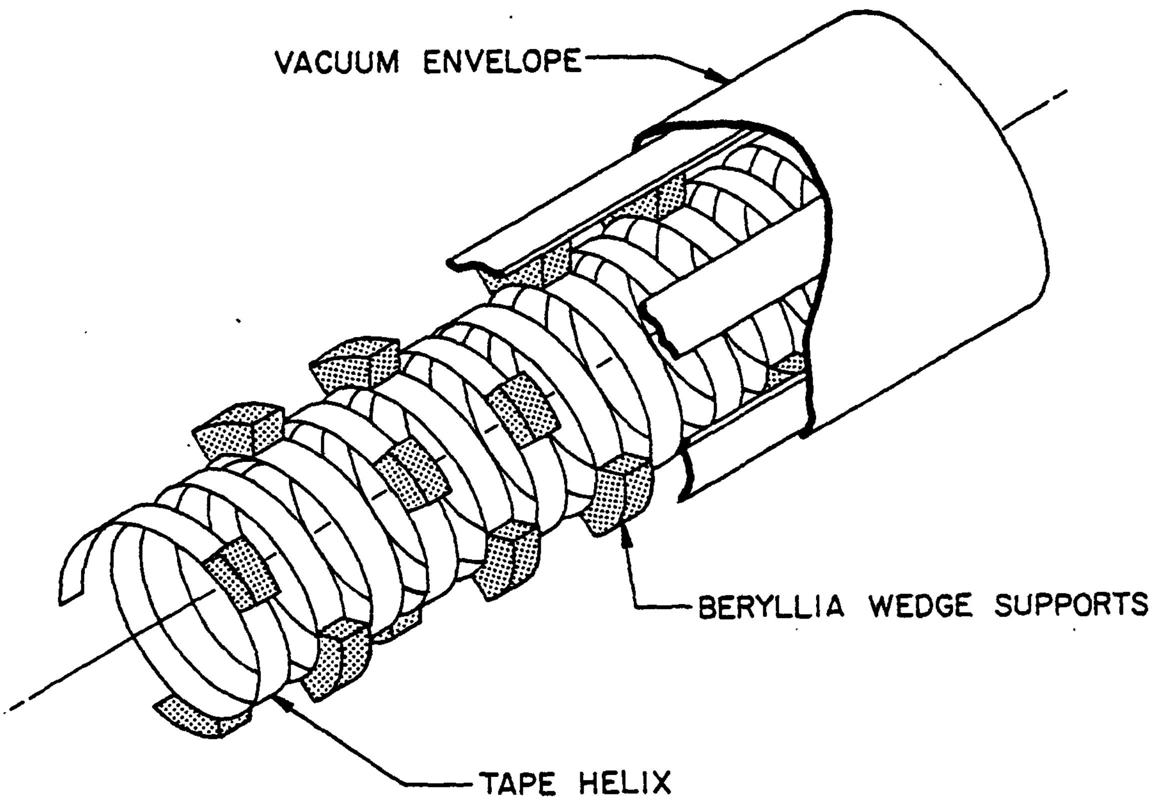


NON-PERIODIC HELIX STRUCTURE

FIGURE 2

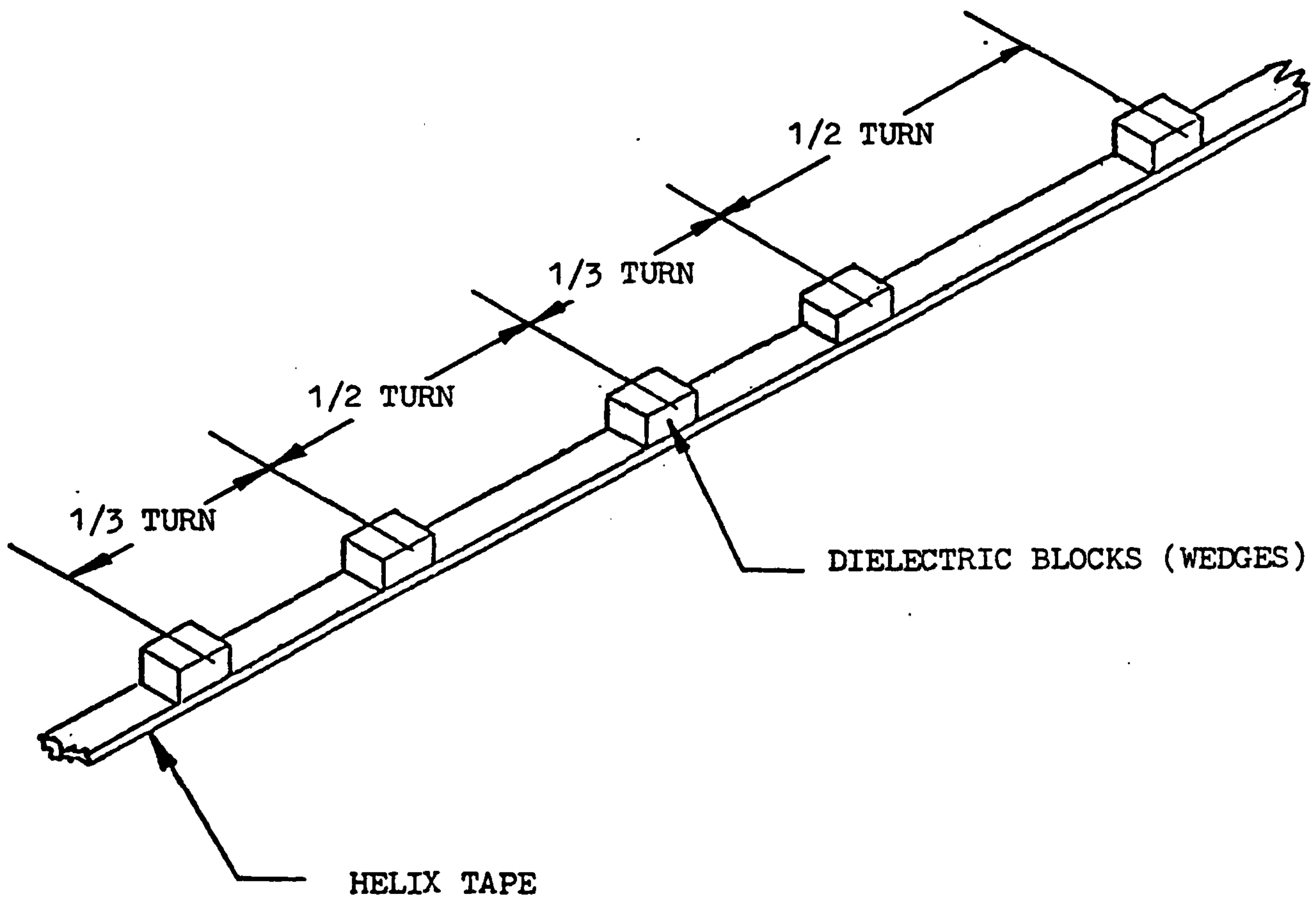


UNWOUND TAPE FOR NON-PERIODIC HELIX

FIGURE 3

2.1 Introduction and Stopband Requirements (continued)

the instability region. An additional advantage of this technique is that it is easier to fabricate than the first technique. Actual drawings of the helix and ladder assemblies used are shown in Figures 4 and 5.

The presence of a stopband in the circuit resulting from the second technique is predicted by calculations described below.

## 2.2 Asymmetric Loading of Periodic Transmission Lines

### 2.2.1 Equivalent Circuit Analysis

The propagation characteristics of helix interaction circuits can be represented by an equivalent circuit of periodically-loaded transmission lines. (References 1 through 5)

The voltage and current of a four-terminal network may be shown by the following relationship.

$$V_1 = A\ V_2 + B\ I_2$$
$$I_1 = C\ V_2 + D\ I_2 \qquad (1)$$

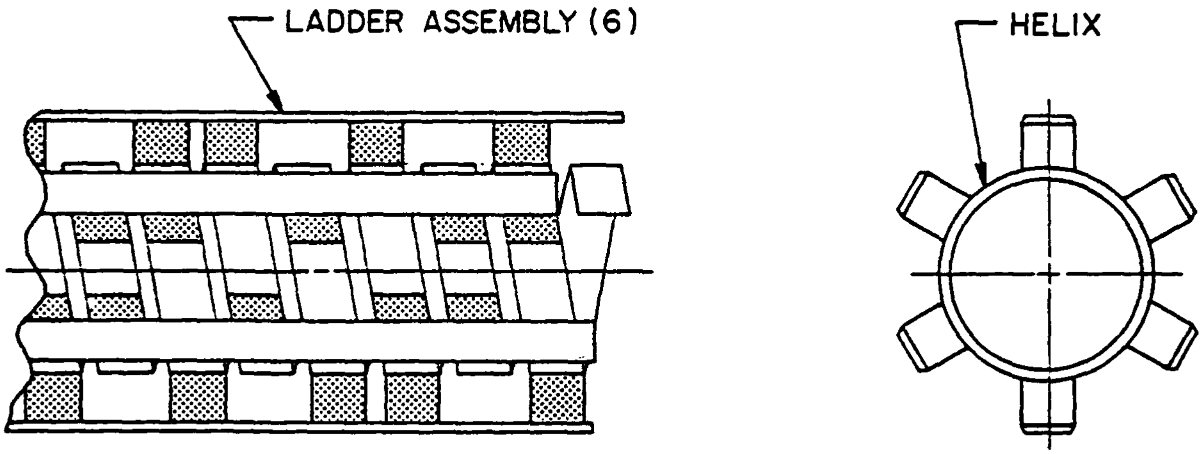


TYPICAL HELIX ASSEMBLY

FIGURE 4

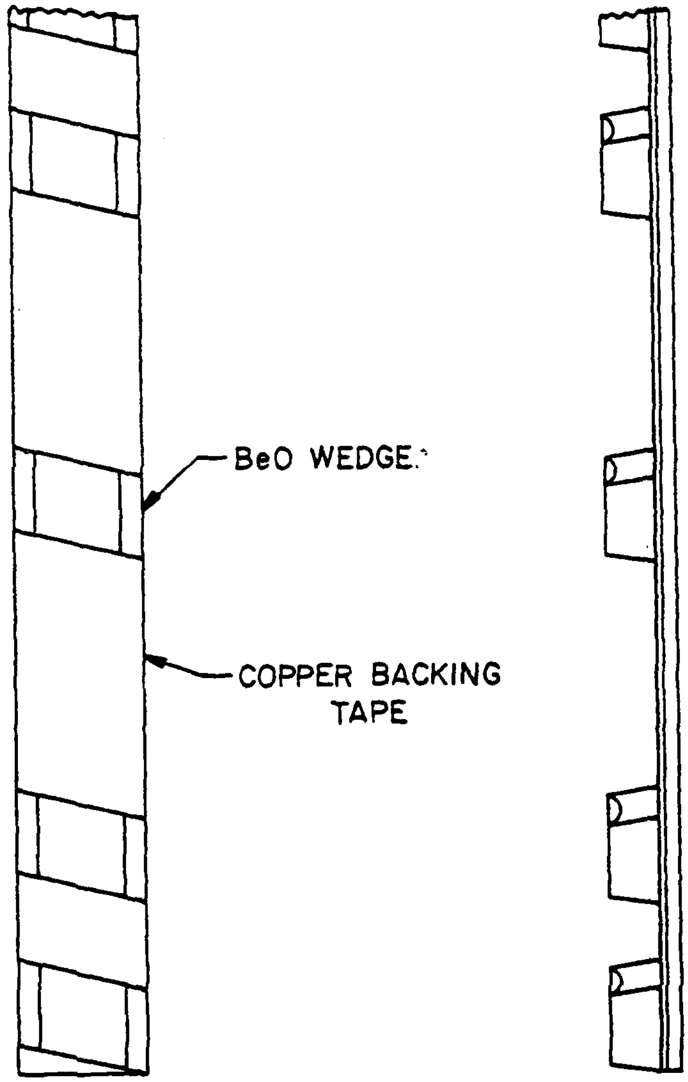


TYPICAL LADDER ASSEMBLY

FIGURE 5

## 2.2.1 Equivalent Circuit Analysis (continued)

where $V_1$, $I_1$ = Input voltage and current

$V_2$, $I_2$ = Output voltage and current

A,B,C,D= Circuit constants

The circuit constants of a few simple networks are shown in Table I.

## 2.2.2 Cascaded Networks

The above equation (1) can be written in a matrix form as

$$\begin{pmatrix} V_1 \\ I_1 \end{pmatrix} = \begin{pmatrix} A & B \\ C & D \end{pmatrix} \begin{pmatrix} V_2 \\ I_2 \end{pmatrix} \qquad (2)$$

Then more general networks can be represented by cascading a number of simple networks as

$$\begin{pmatrix} V_1 \\ I_1 \end{pmatrix} = \begin{pmatrix} M_n \end{pmatrix} \begin{pmatrix} V_n \\ I_n \end{pmatrix} \qquad (3)$$

where

$$\begin{pmatrix} M_n \end{pmatrix} = \begin{pmatrix} M_1 \end{pmatrix} \begin{pmatrix} M_2 \end{pmatrix} \begin{pmatrix} M_3 \end{pmatrix} \cdots \begin{pmatrix} M_{n-1} \end{pmatrix}$$
$$= \begin{pmatrix} A_n & B_n \\ C_n & D_n \end{pmatrix}$$

$$\begin{pmatrix} V_1 \\ I_1 \end{pmatrix} = M_1 \cdot M_2 \cdot M_3 \cdots M_{n-1} \cdot \begin{pmatrix} V_n \\ I_n \end{pmatrix}$$

$$M_n = \begin{pmatrix} A_n & B_n \\ C_n & D_n \end{pmatrix}$$

where

$V$ = INPUT / OUTPUT VOLTAGE

$I$ = INPUT / OUTPUT CURRENT

$M_n$ = MATRIX OF GENERAL CIRCUIT PARAMETERS

A,B,C,D = GENERAL CIRCUIT PARAMETERS

| | TRANSMISSION LINE | SERIES ELEMENT | SHUNT ELEMENT |
|---|---|---|---|
| | 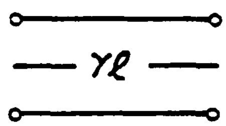  | 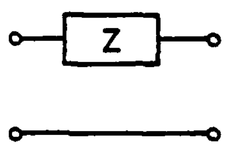  | 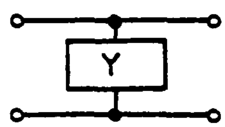  |
| A | COSH ($\gamma\ell$) | 1 | 1 |
| B | $Z_0$ SINH ($\gamma\ell$) | Z | 0 |
| C | $\frac{1}{Z_0}$ SINH ($\gamma\ell$) | 0 | Y |
| D | COSH ($\gamma\ell$) | 1 | 1 |

TABLE I

GENERAL CIRCUIT PARAMETERS FOR CASCADED NETWORKS

2.2.2 Cascaded Networks (continued)

If an equivalent transmission line is assumed to represent the same characteristics as the cascaded network,

$$A_n = \cosh(\gamma \ell)$$

$$B_n = Z \sinh(\gamma \ell)$$

$$C_n = Y \sinh(\gamma \ell)$$

$$D_n = \cosh(\gamma \ell)$$

where

$$\gamma = \alpha + j\beta$$

The propagation constant $\gamma$ can be determined from the above equations by separating the circuit constant into a real part and an imaginary part.

$$A_n = P + jQ$$

$$\cosh(\gamma \ell) = \cosh(\alpha \ell) \cos(\beta \ell) + j \sinh(\alpha \ell) \sin(\beta \ell)$$

Then

$$P = \cosh(\alpha \ell) \cos(\beta \ell)$$

$$Q = \sinh(\alpha \ell) \sin(\beta \ell)$$

These equations can be solved to obtain

$$\cosh^2(\alpha \ell) = \left\{(1+P^2+Q^2) \pm \sqrt{(1-P^2-Q^2)^2+4Q^2}\right\} / 2$$

$$\cos^2(\beta \ell) = P^2/\cosh^2(\alpha \ell)$$

Thus

$\alpha$ and $\beta$ can be found from P and Q.

2.2.3 Computations

A computer program /BLOCK/ was prepared by using the equations described above. A number of cases with various circuit configurations are computed to study their transmission characteristics. Principal parameters related to these computations are

$p$ = Periodic length of the circuit

$Y_n$ = Normalized loading susceptance

$N$ = Number of $Y_n$ per periodic length

$R$ = Circuit loss per periodic length, db

$\beta$ = Phase constant of the circuit

$X$ = Normalized phase shift per periodic length, $\frac{\beta P}{\pi}$

The phase velocity of the circuit is assumed to be constant over the frequency range without the loading. The loading susceptance is assumed to be in the following form.

$$Y_n = j\omega C_n$$

where

$\omega$ = angular frequency

$C$ = Equivalent loading capacitance

Figure 6 shows the most simple case with one loading element per periodic length on a lossless circuit. The loading is symmetric with respect to the helix. The stop bands are created at every integer value of X. When the

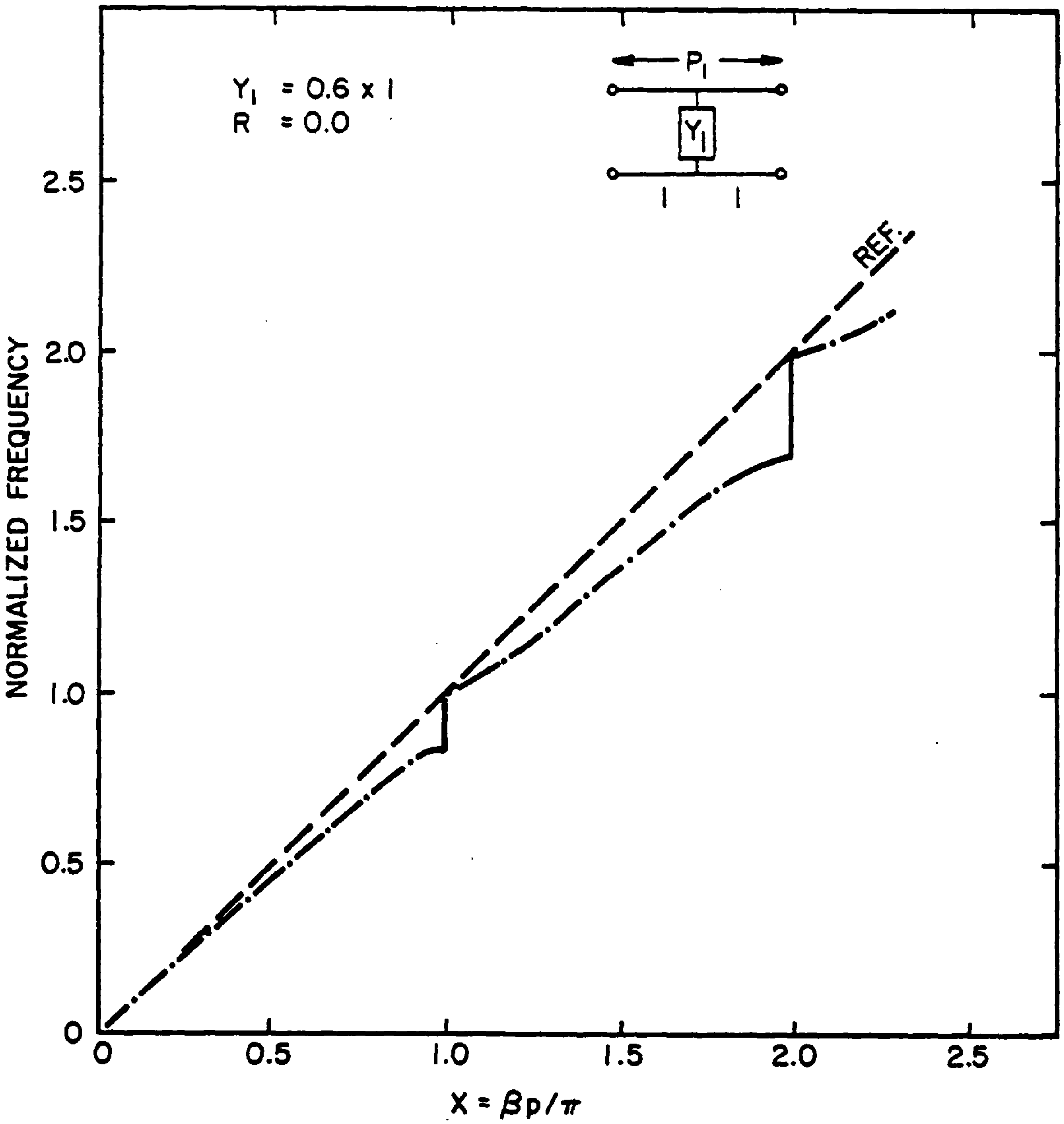


COMPUTED STOPBANDS FOR A LOSSLESS SYMMETRIC CIRCUIT WITH ONE SUSCEPTANCE PER PERIOD

FIGURE 6

2.2.3 Computations (continued)

number of loading elements is increased to two per periodic length, the computed $\omega$-$\beta$ diagram is shown in Figure 7, where the stopbands are located at integer multiples of $X = 2.0$. One can infer then that for n loading elements per periodic length, the stopbands will occur at integer multiples of $X = n$. However, if an additional perturbation is added with a frequency of one per periodic length, stopbands will appear at integer values of X, as shown in Figure 8.

When finite circuit loss is assumed, the transmission characteristics are modified and the results are shown in Figure 9 with expanded scale near $X = 1.0$. The similar computations with finite circuit loss when the loading susceptances are reduced by one half are plotted in Figure 10. Figures 9 and 10 indicate that the magnitude of the stopband and the maximum attenuation in the stopband are functions of the loading susceptance, as plotted in Figure 11.

Figure 12 shows the computed $\omega$-$\beta$ diagram when one of three loading capacitances is higher than the other two for each periodic length. The similar case with varied loading capacitance is plotted in Figure 13 with expanded scale near $X = 1.0$.

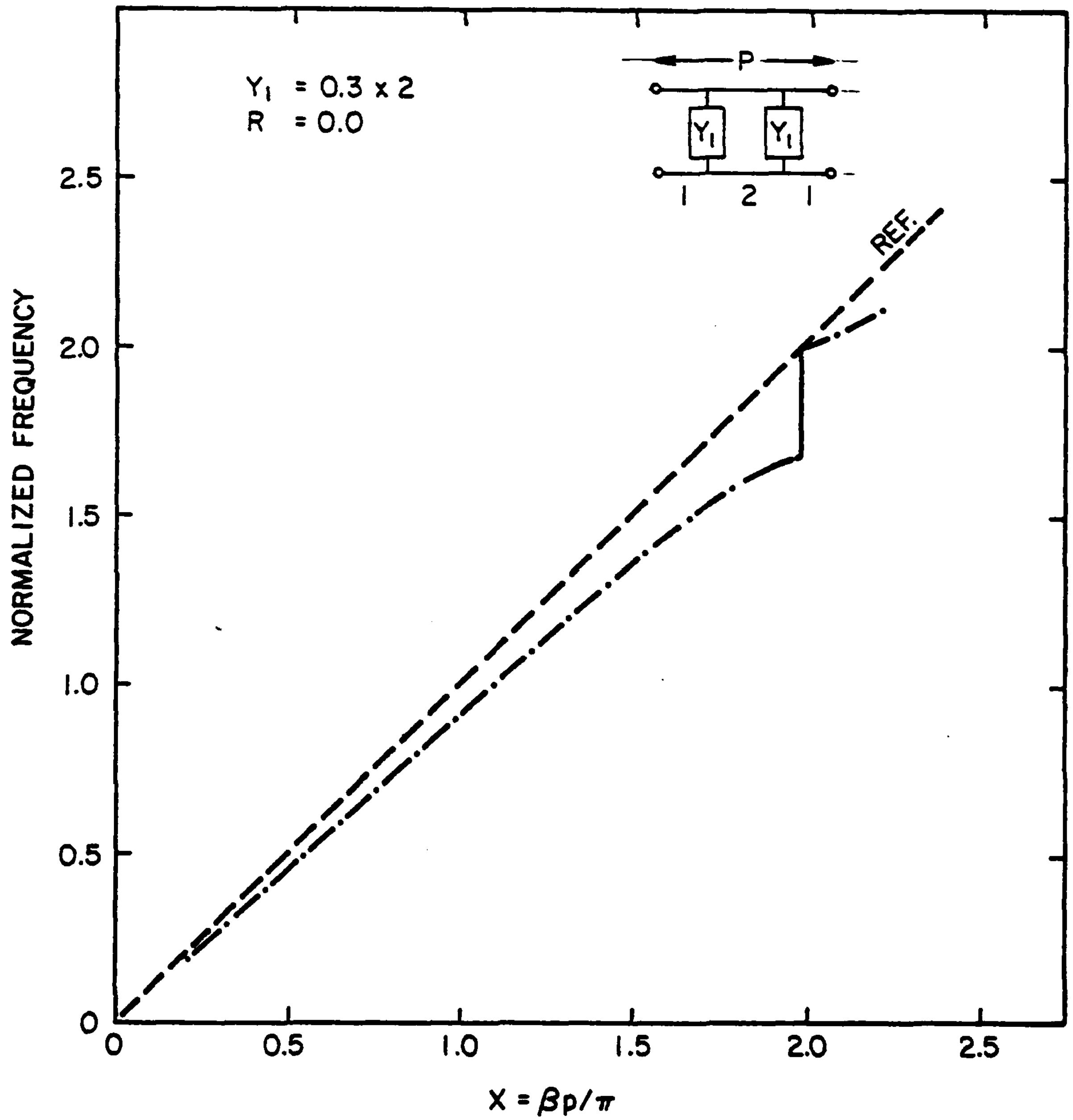


COMPUTED STOPBANDS FOR A LOSSLESS SYMMETRIC CIRCUIT WITH TWO SUSCEPTANCES PER PERIOD

FIGURE 7

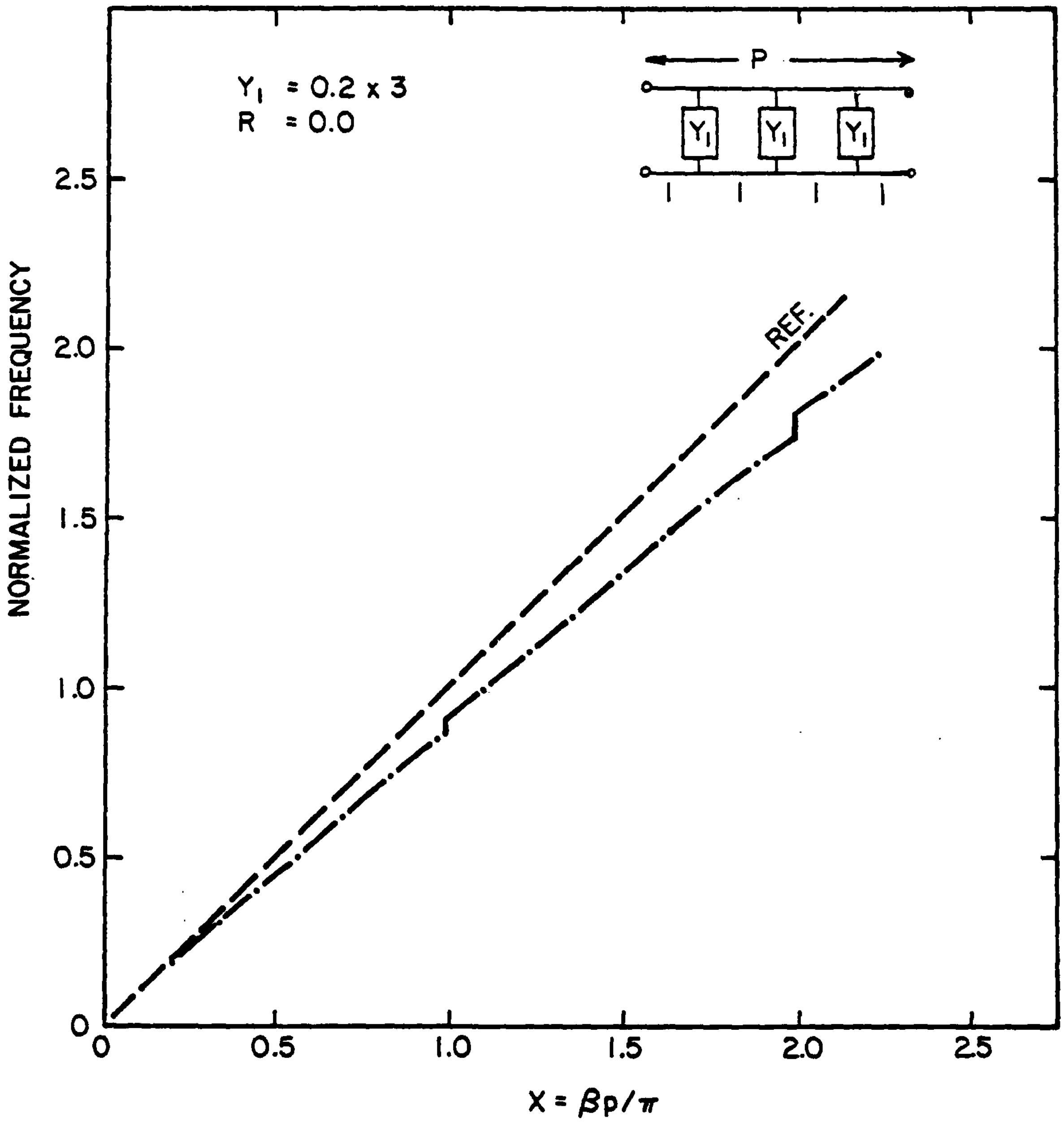


COMPUTED STOPBANDS FOR A LOSSLESS SYMMETRIC CIRCUIT WITH THREE SUSCEPTANCES PER PERIOD

FIGURE 8

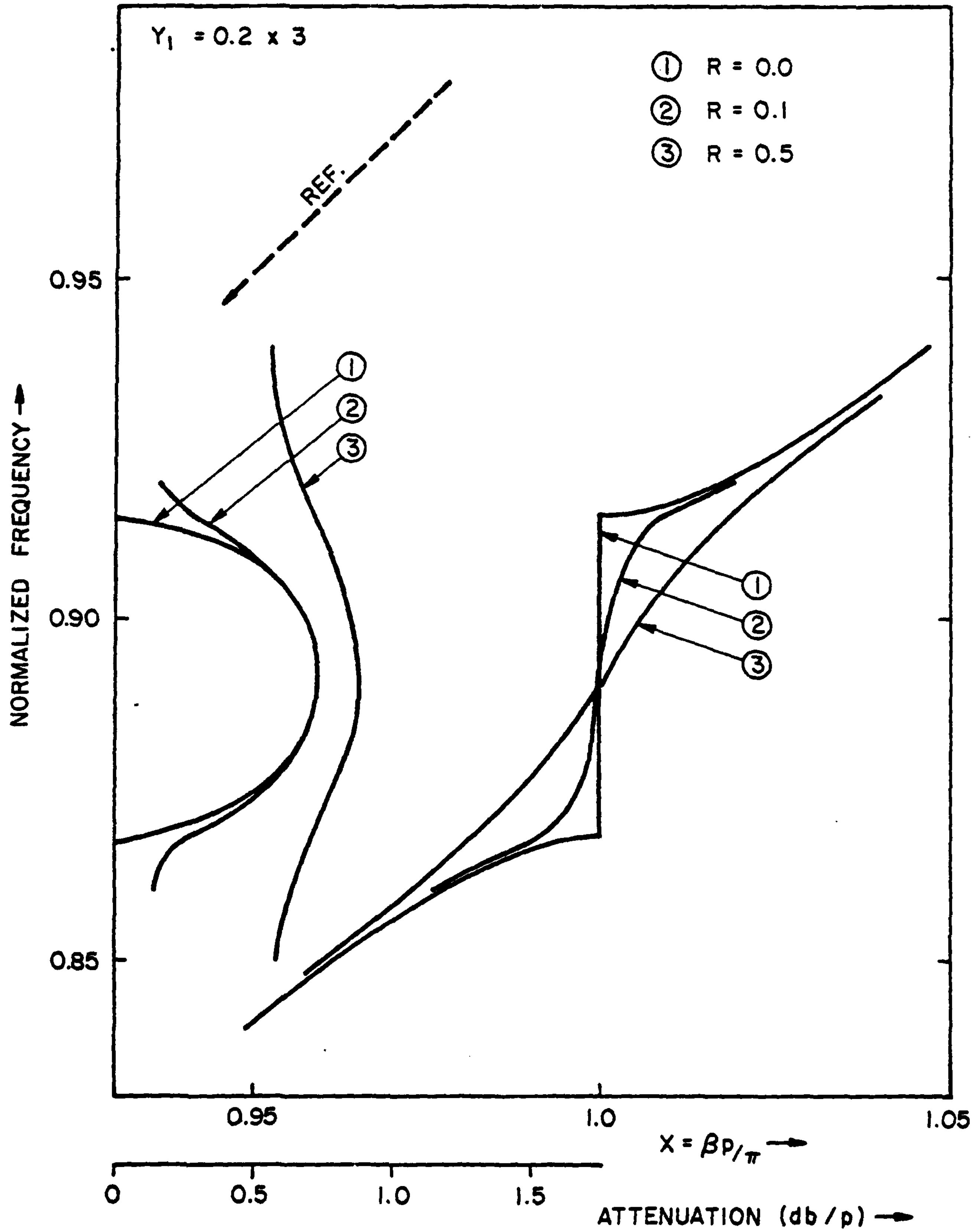


COMPUTED STOPBANDS AND CIRCUIT ATTENUATION DUE TO SYMMETRIC LOADING SUSCEPTANCES WITH CIRCUIT LOSS

FIGURE 9

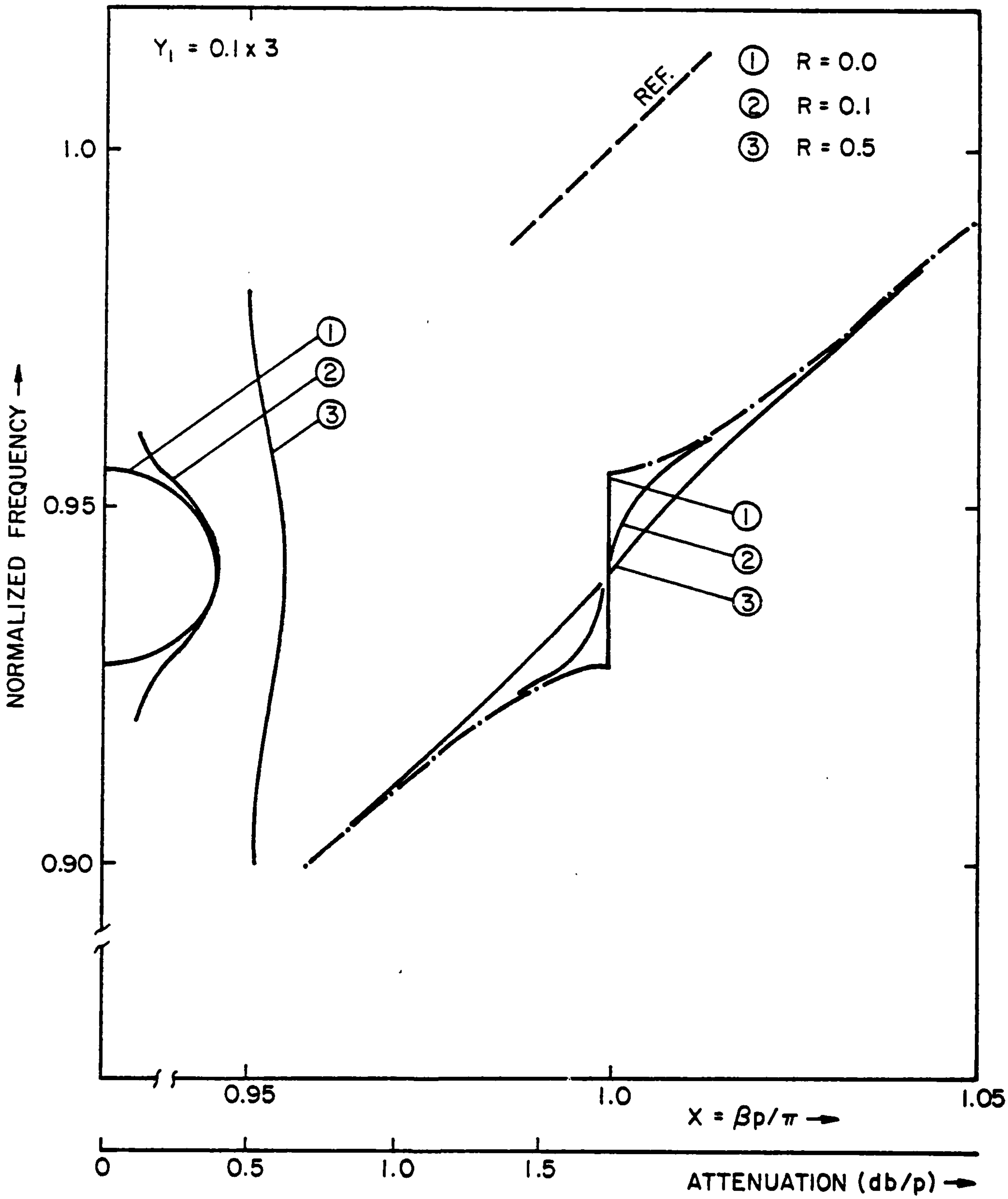


COMPUTED STOPBANDS AND CIRCUIT ATTENUATION DUE TO SYMMETRIC LOADING SUSCEPTANCES WITH CIRCUIT LOSS

FIGURE 10

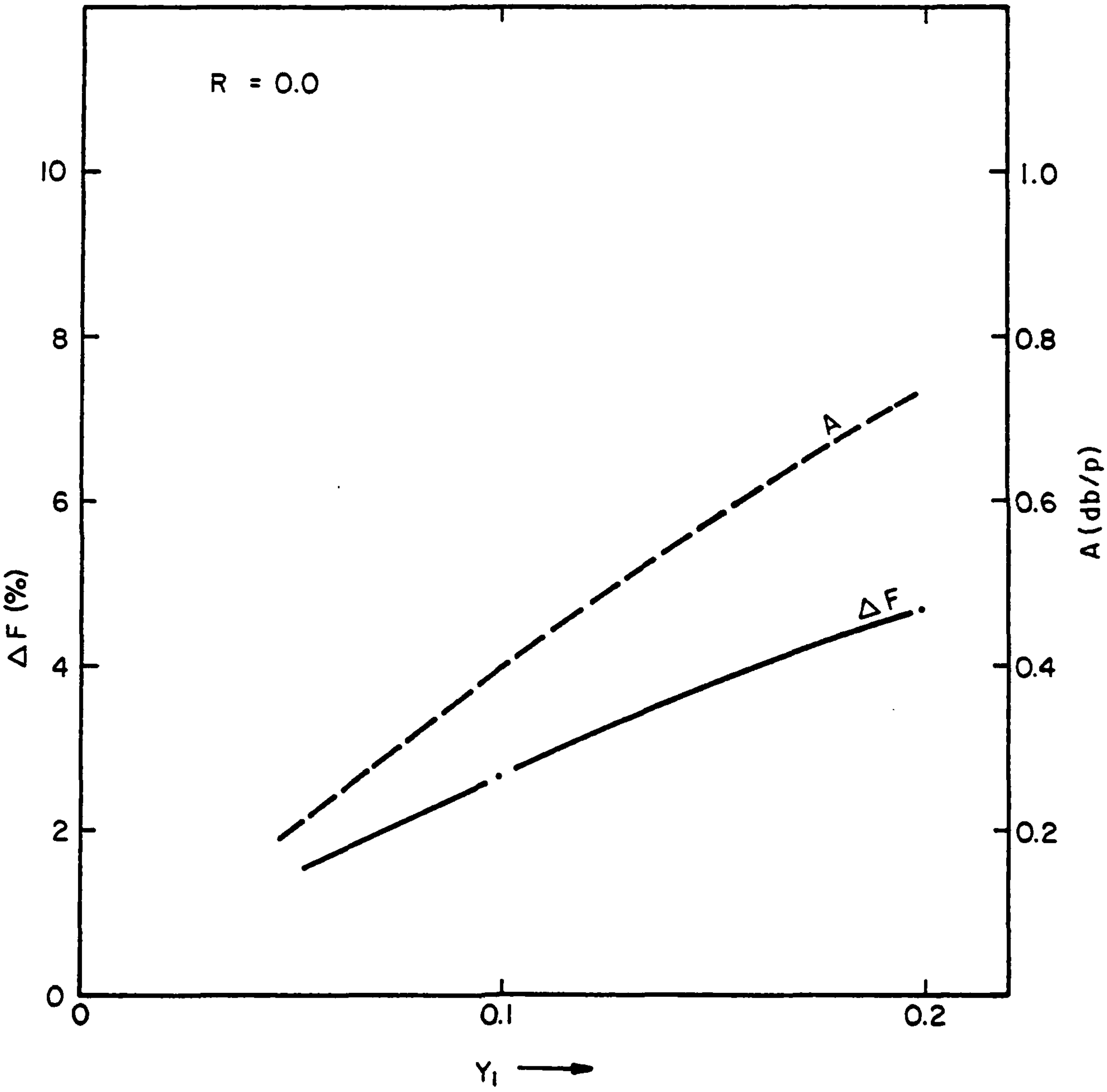


STOPBAND MAGNITUDE AND MAXIMUM STOPBAND ATTENUATION
AS A FUNCTION OF LOADING SUSCEPTANCE

FIGURE 11

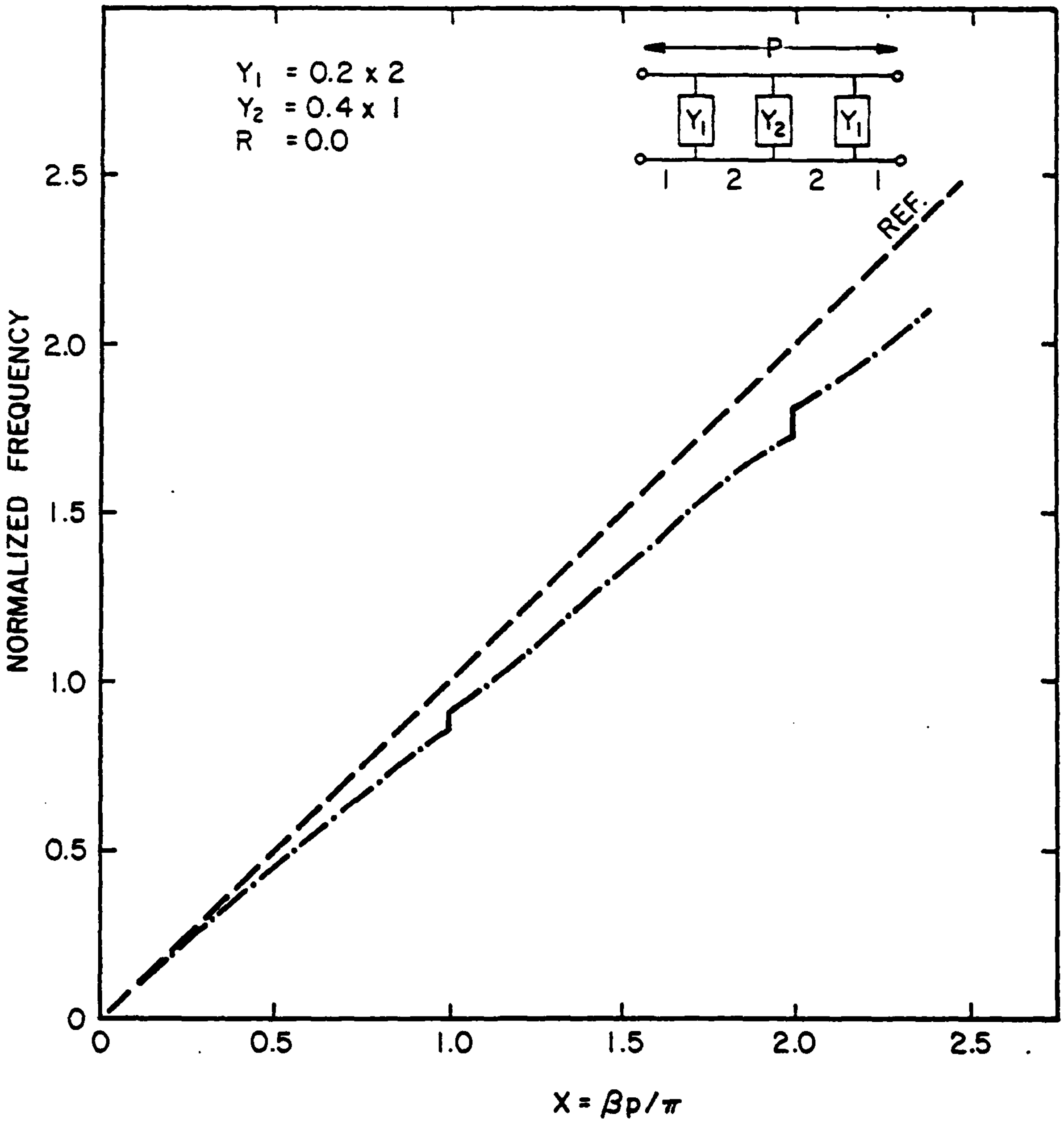


COMPUTED STOPBANDS DUE TO ASYMMETRICAL LOADING SUSCEPTANCES

FIGURE 12

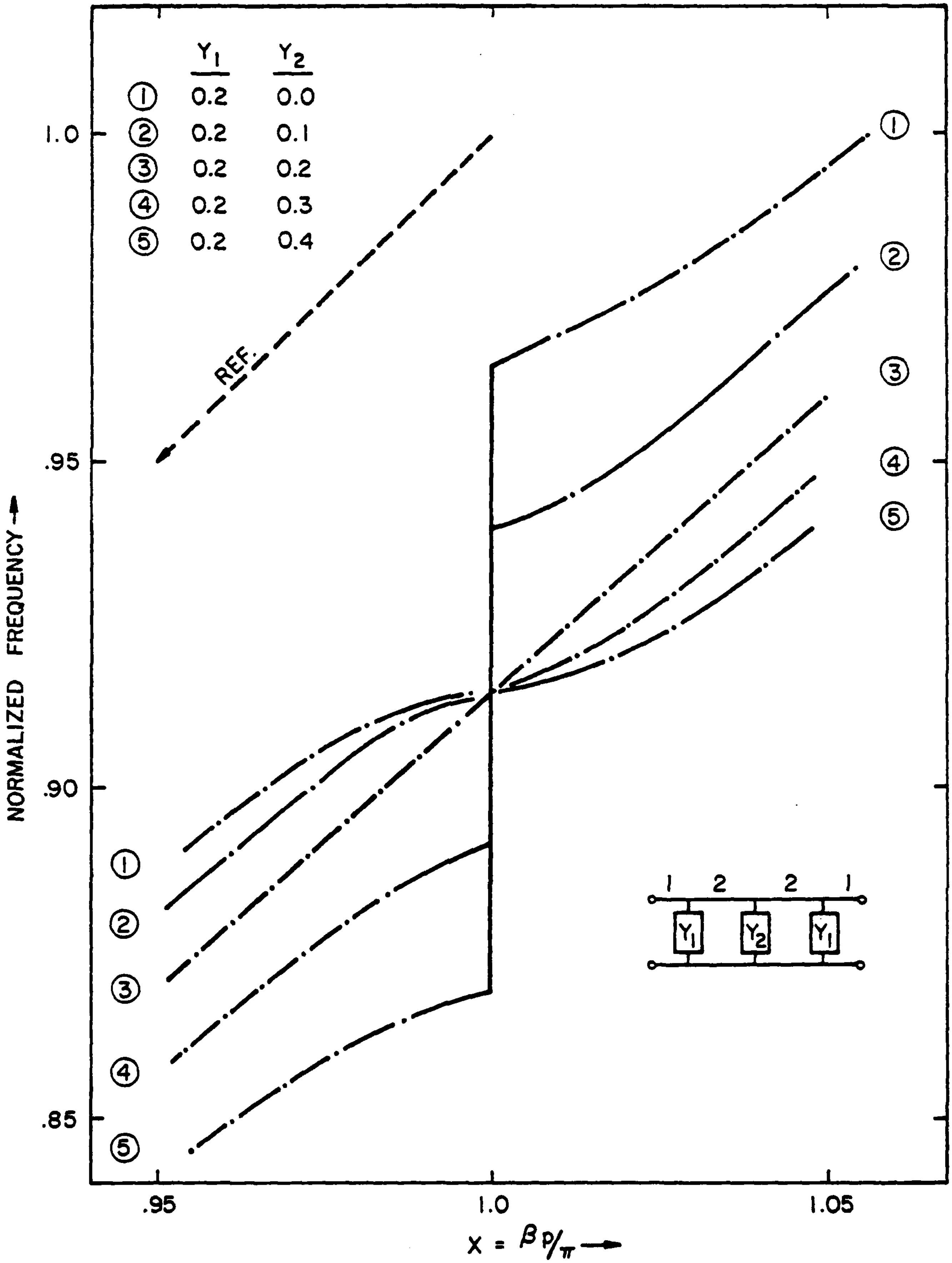


COMPUTED STOPBANDS DUE TO UNEQUAL LOADING SUSCEPTANCES

FIGURE 13

2.2.3 Computations (continued)

It can be determined from these plots that the location and bandwidth of the stopbands are functions of the magnitude and position of the loading elements. Asymmetry is caused by displacement of the loading elements from turn to turn.

2.2.4 Proposed Circuits

Two possible circuits with non-periodic or asymmetrical loading are compared to the conventional circuit in Figure 14. The periodic length q of these test circuits is a little shorter than the periodic length p of the helix, which will create a stopband in the frequency range where backward-wave oscillations are expected.

Computed $\omega$-$\beta$ diagrams are shown for these circuits in Figures 15 and 16, in which the amount of loading susceptance is varied. It can be seen in these figures that both circuits have similar transmission characteristics except circuit (3) has a slightly higher phase velocity than circuit (2), because the total amount of loading in circuit (3) is less than that of circuit (2). However, the thermal properties of circuit (2) are superior to those of circuit (3). Therefore, circuit (1)

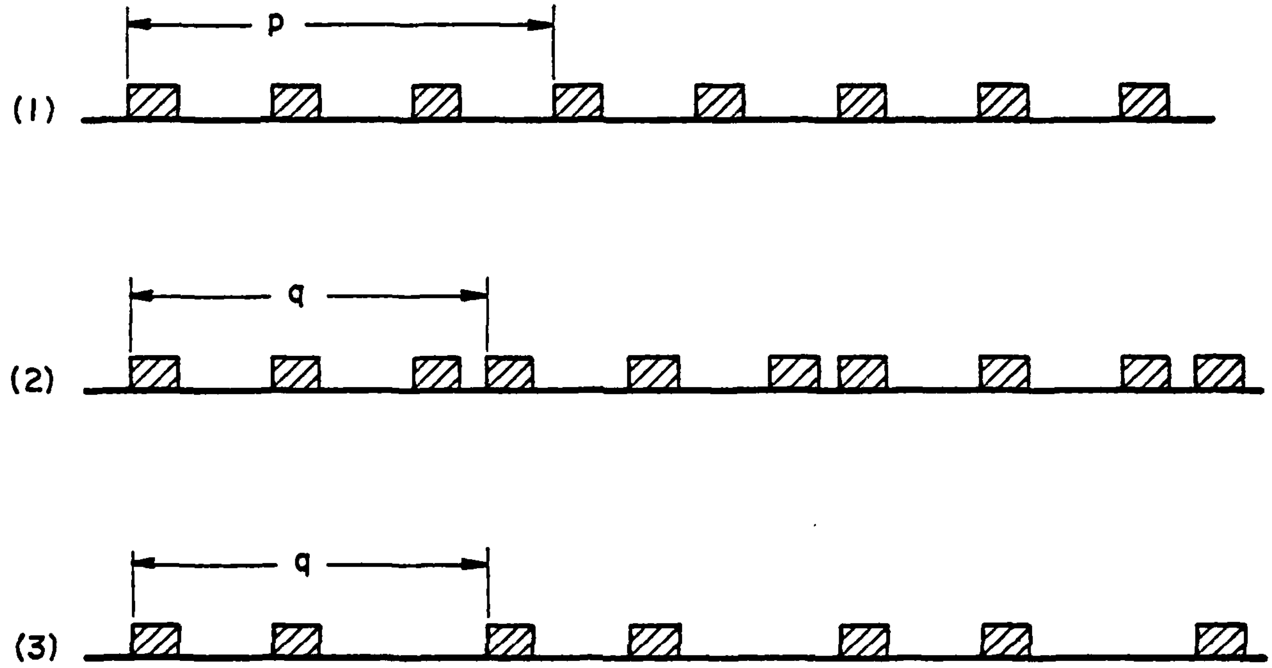


(1) SYMMETRIC LOADING WITH EQUAL INTERVALS.

(2) ASYMMETRIC LOADING WITH PERIODICALLY REDUCED INTERVALS AND INCREASED LOADING.

(3) ASYMMETRIC LOADING WITH PERIODICALLY REDUCED INTERVALS AND DECREASED LOADING.

THREE TYPES OF BLOCK-SUPPORTED HELIX WITH DIFFERENT LOADING ARRANGEMENT

FIGURE 14

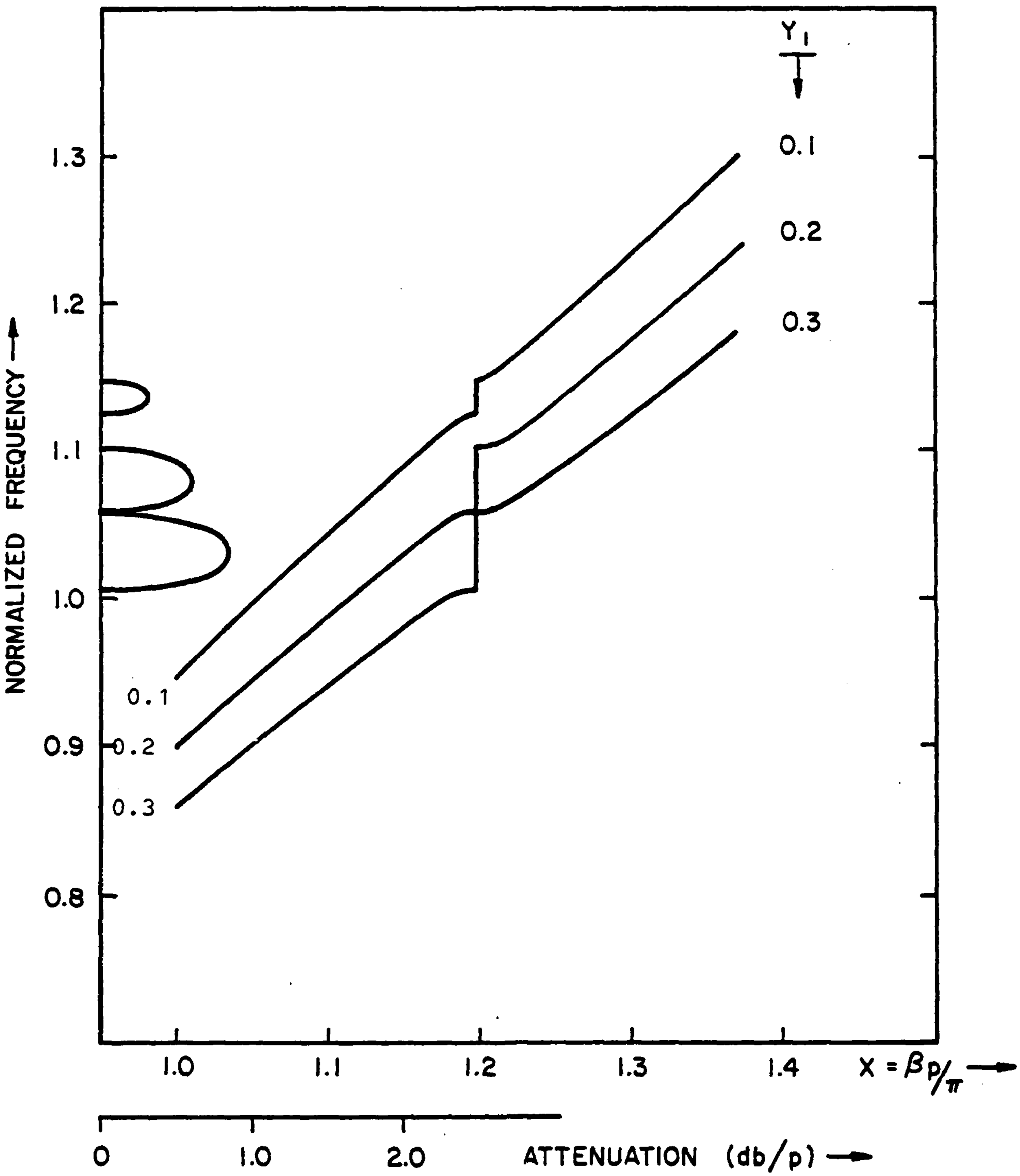


COMPUTED STOPBANDS FOR BLOCK SUPPORTED
HELIX WITH ASYMMETRIC LOADING

FIGURE 15

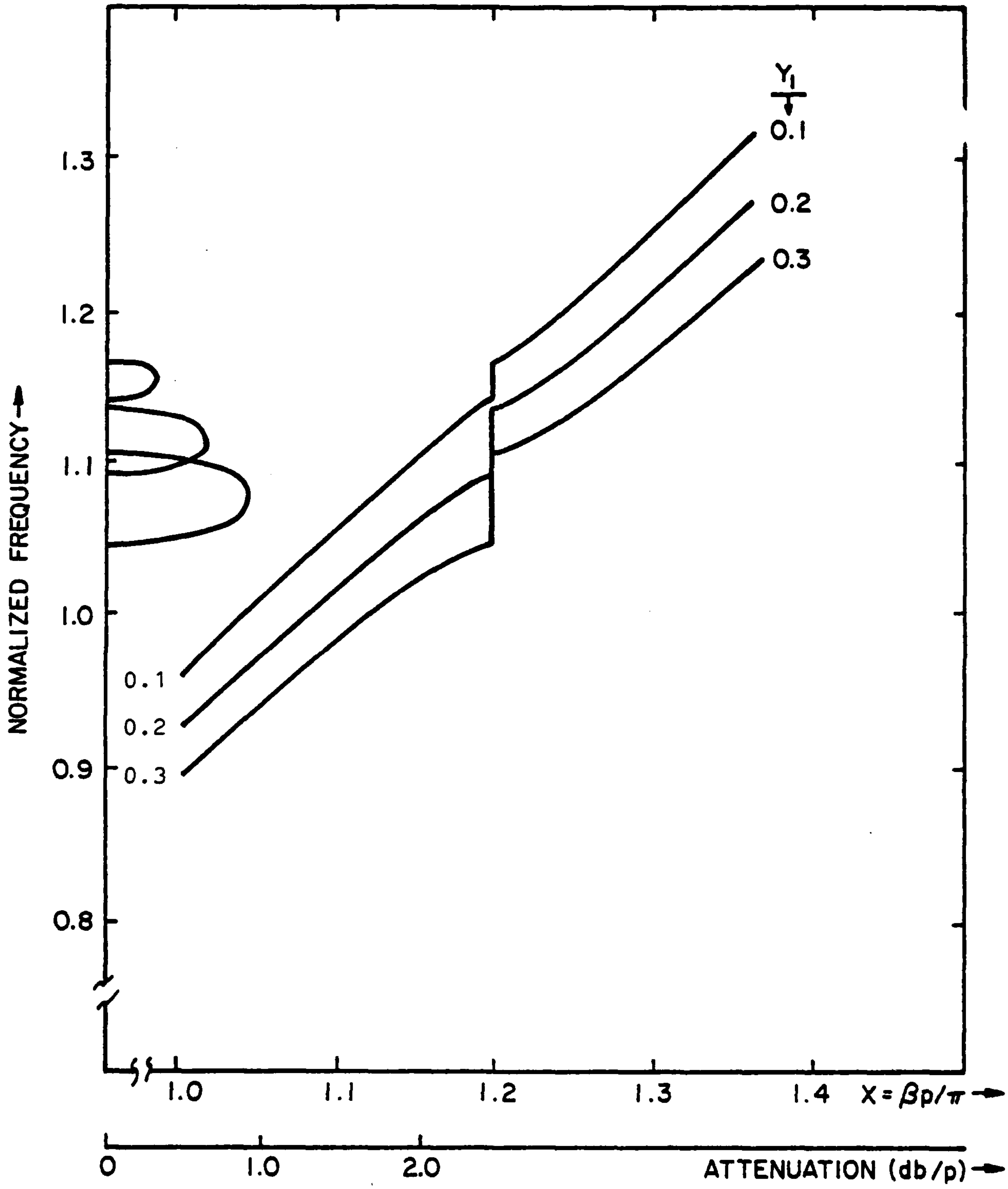


COMPUTED STOPBANDS FOR BLOCK SUPPORTED HELIX
WITH ASYMMETRIC LOADING

FIGURE 16

2.2.4 Proposed Circuits (continued)

was used in the cold and hot tests.

## 2.3 Cold Tests

The first cold test circuit built, using stycast wedges with a dielectric constant of 6.0 to simulate BeO, had a loading period which was 7/6 of the pitch, instead of 5/6, as was intended. Despite the fact that this circuit was not useful in a tube, information obtained from it was considered very useful, as it helped to determine whether or not the circuit analysis was correct. Therefore, the circuit was thoroughly analyzed and some conclusions were made relative to it.

In Figure 17, the circuit velocity of the fundamental forward wave is shown as a function of frequency. The stopbands in this mode are clearly shown as is the change in velocity which occurs near cutoff.

Figure 18 shows the same data in a non-normalized $\omega$-$\beta$ diagram, and Figure 19 shows this data with additional information added based on the assumption that the modes are symmetrical about the line $\frac{\beta p}{\pi} = 1.0$. Figure 20 shows measured circuit impedance as a function of frequency.

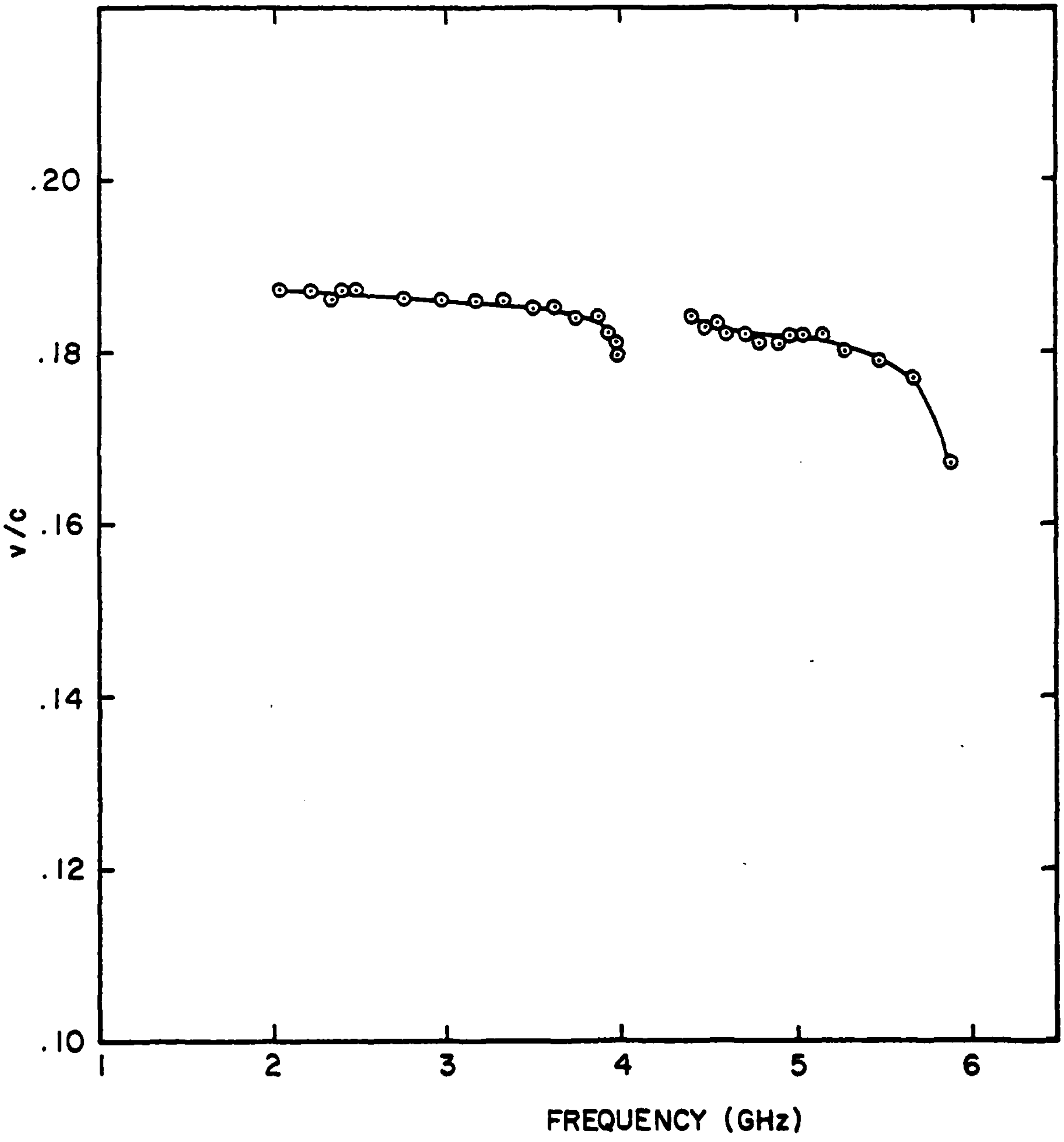


CIRCUIT VELOCITY FOR CIRCUIT WITH LOADING PERIOD = 7/6 PITCH

FIGURE 17

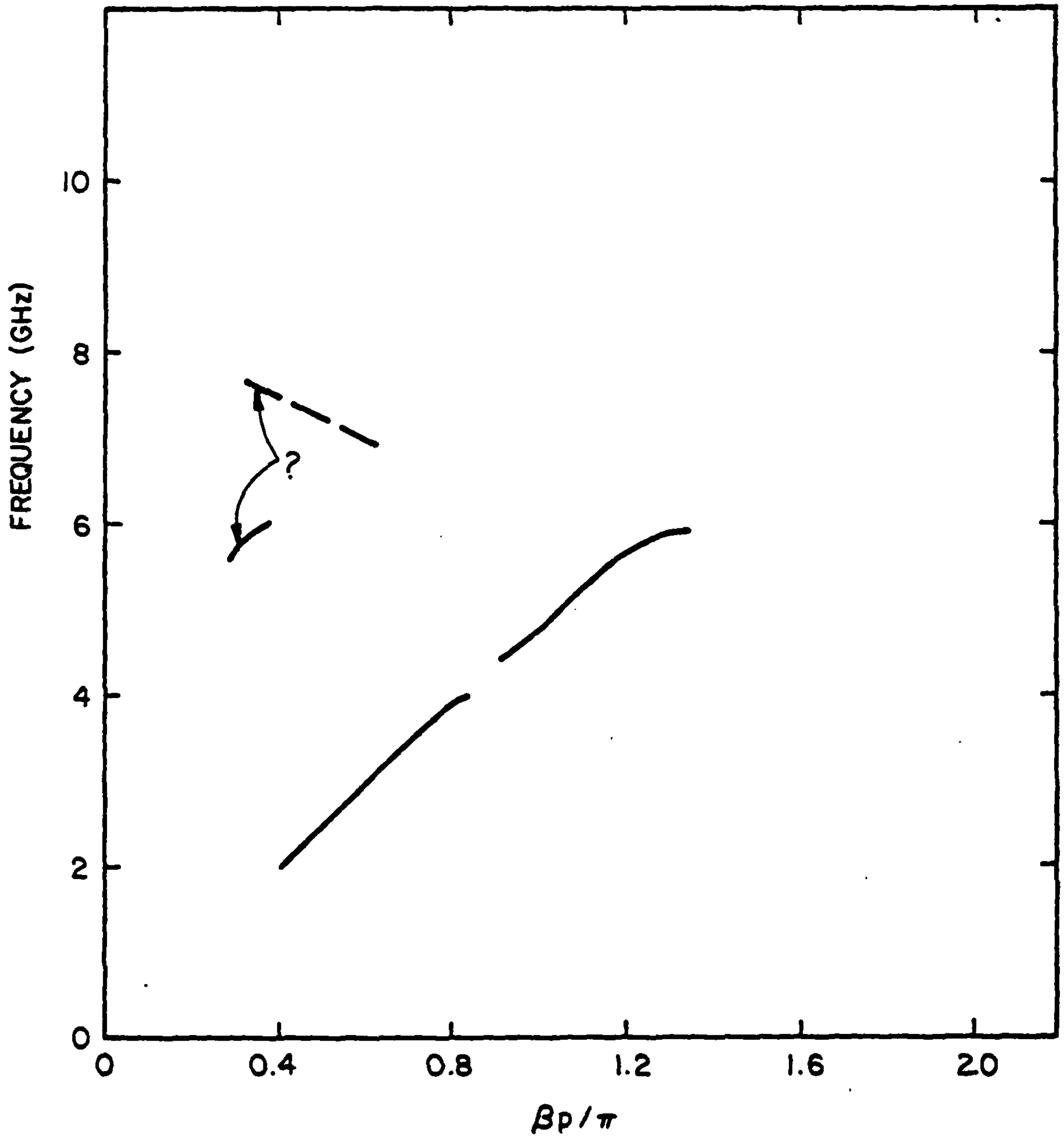


COLD TEST RESULTS FOR CIRCUIT WITH LOADING PERIOD = 7/6 PITCH

FIGURE 18

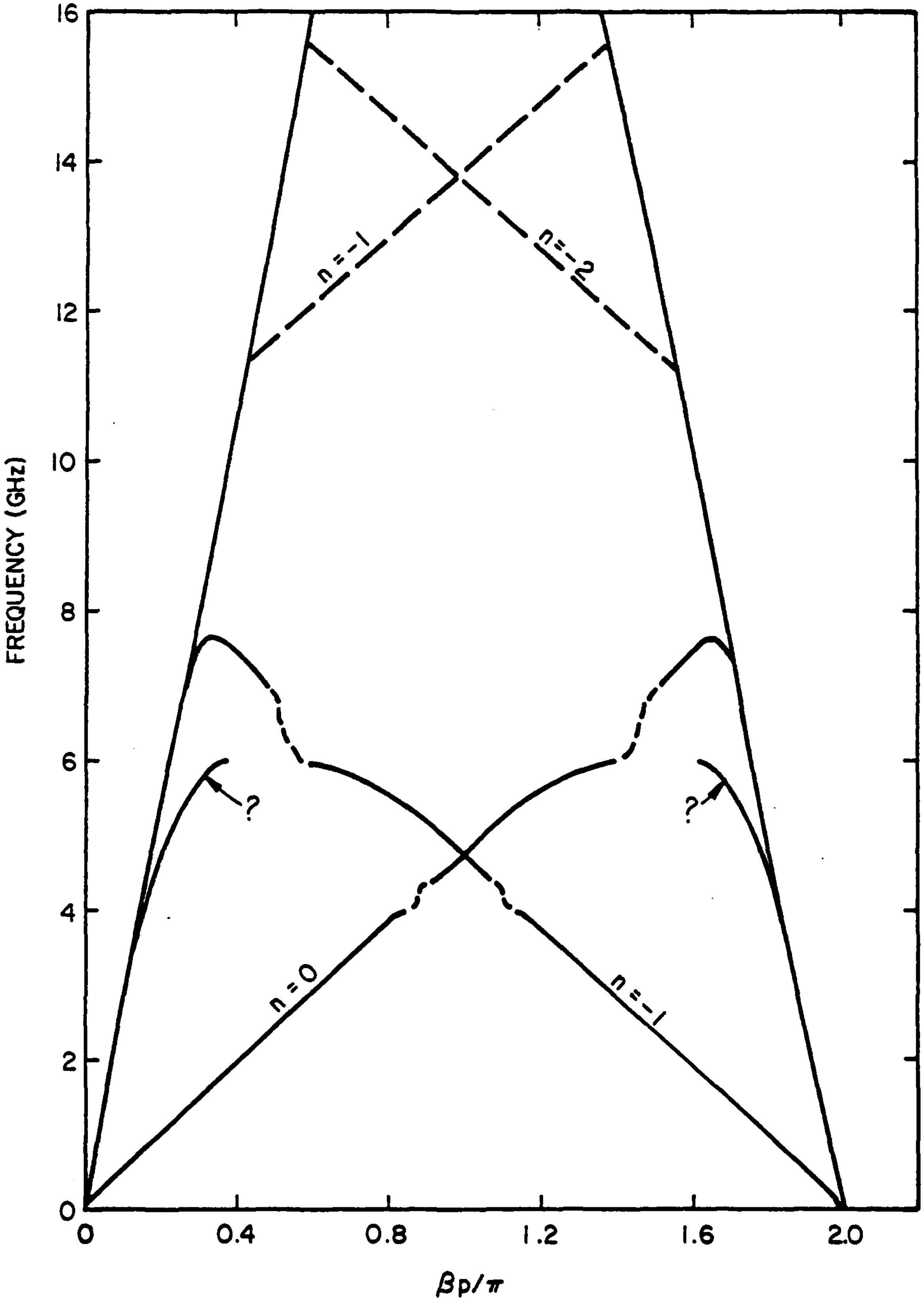


ASSUMED MODE PRESENTATION FOR CIRCUIT WITH LOADING PERIOD = 7/6 PITCH

FIGURE 19

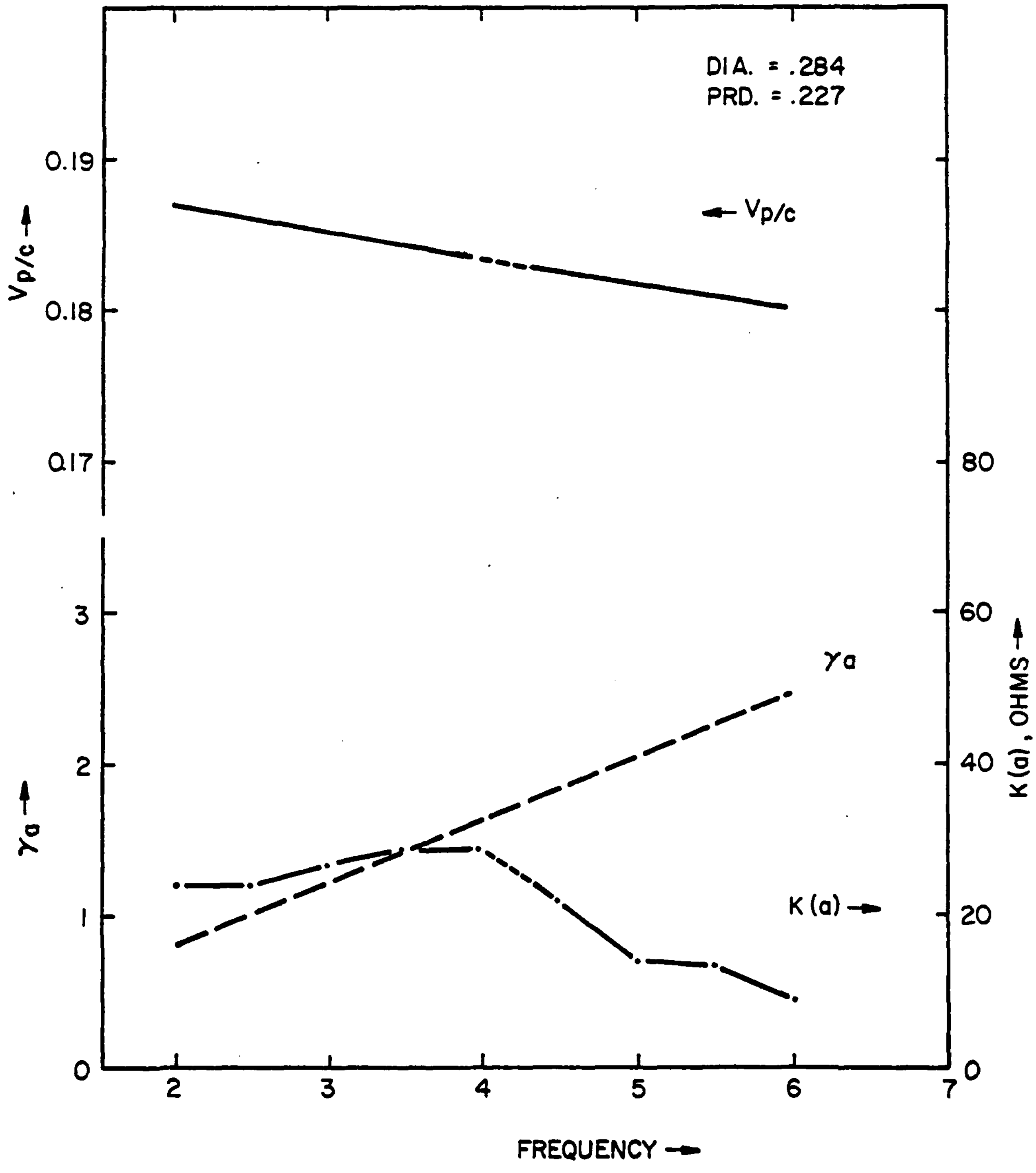


CIRCUIT IMPEDANCE FOR CIRCUIT WITH LOADING PERIOD = 7/6 PITCH

FIGURE 20

## 2.3 Cold Tests

The first stopband occurs at the exact value of $\frac{\beta p}{\pi}$ predicted by the circuit analysis. The sharp cutoff characteristics indicate that the circuit has very low loss per unit length in the transmitting region, which is to be expected with a copper helix. The reason for the existence of the second stopband was not determined. All modes above 5.5 GHz were excited with the metal perturbing bead placed off axis and the responses were weaker above 7 GHz. Since this was not the circuit to be used on the tube, it was dismantled and rebuilt with the 5/6 period, as originally intended.

A second cold test circuit was built using Stycast wedges with a dielectric constant of 6.0. The period of the loading on this circuit was 5/6 of the pitch, as originally intended to produce the correct stopband.

In Figure 21, cold circuit loss is shown as a function of frequency. The pass and stopbands are clearly indicated. The higher pass bands were also present on the earlier test device, however, in this case we were unsuccessful in our attempt to excite any modes in these bands even

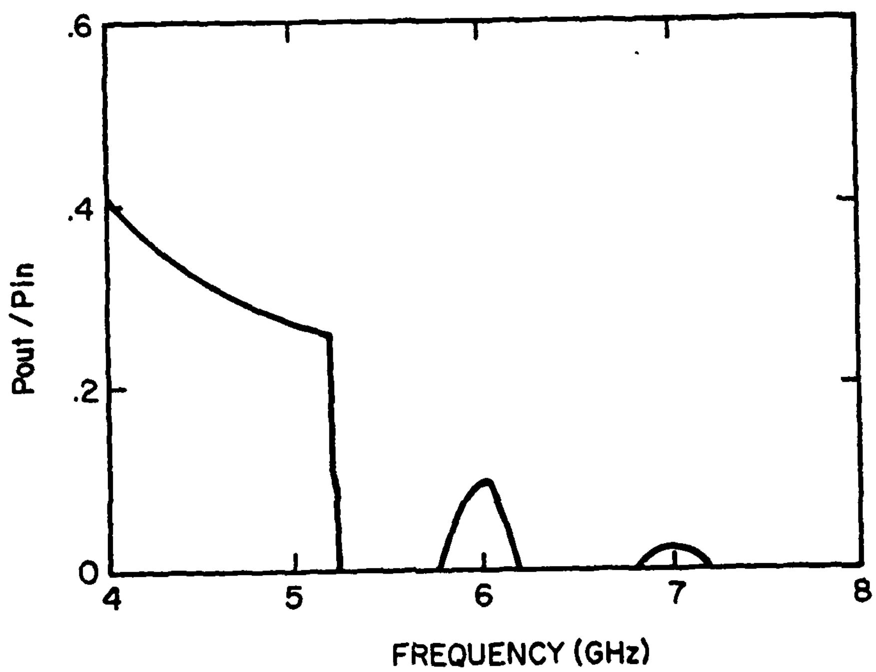


COLD CIRCUIT TRANSMISSION FOR CIRCUIT
WITH LOADING PERIOD = 5/6 PITCH

FIGURE 21

2.3 Cold Tests (continued)

with the perturbing bead off-axis.

In Figure 22, the circuit velocity of the fundamental forward wave is shown as a function of frequency. This circuit is slightly slower and more dispersive than the circuit with a loading period that is 7/6 of the pitch, as described in Section 2.2. This is due to the fact that the dielectric loading is greater as a result of the change in period.

Figure 23 shows the same data in a non-normalized $\omega$-$\beta$ diagram. The -1 space harmonic is also shown. Figure 24 shows measured circuit impedance as a function of frequency.

## 2.4 Hot Test Vehicle

The tube used on this program is the L-5708-50. This tube was expected to operate over an octave band centered at 3.5 GHz, with nominal output power of 10 kW. Almost all of the parts for this tube came from an existing design, the L-5565. The major changes had to do with the circuit. Besides the use of the non-periodic helix, the circuit

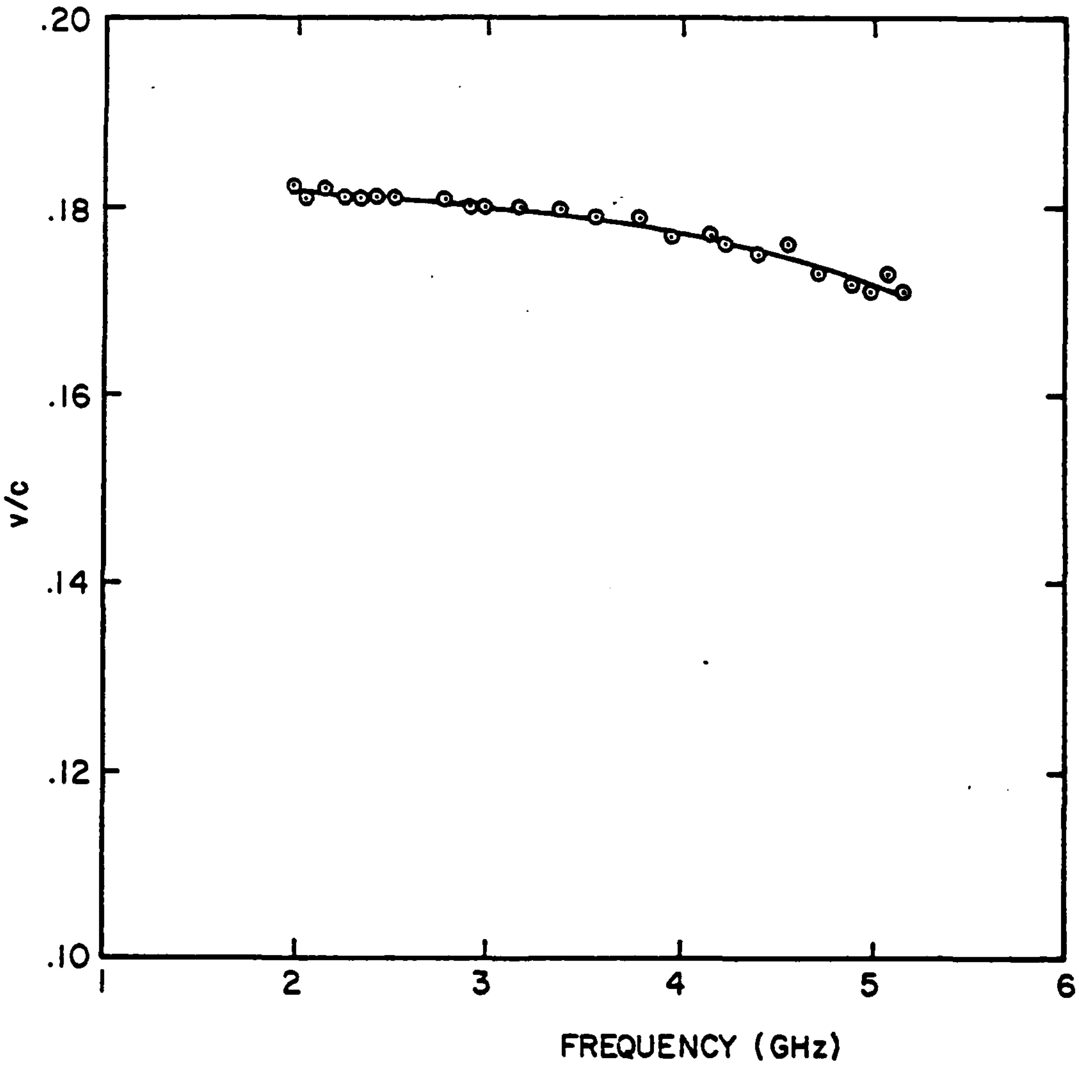


CIRCUIT VELOCITY FOR CIRCUIT WITH LOADING PERIOD = 5/6 PITCH

FIGURE 22

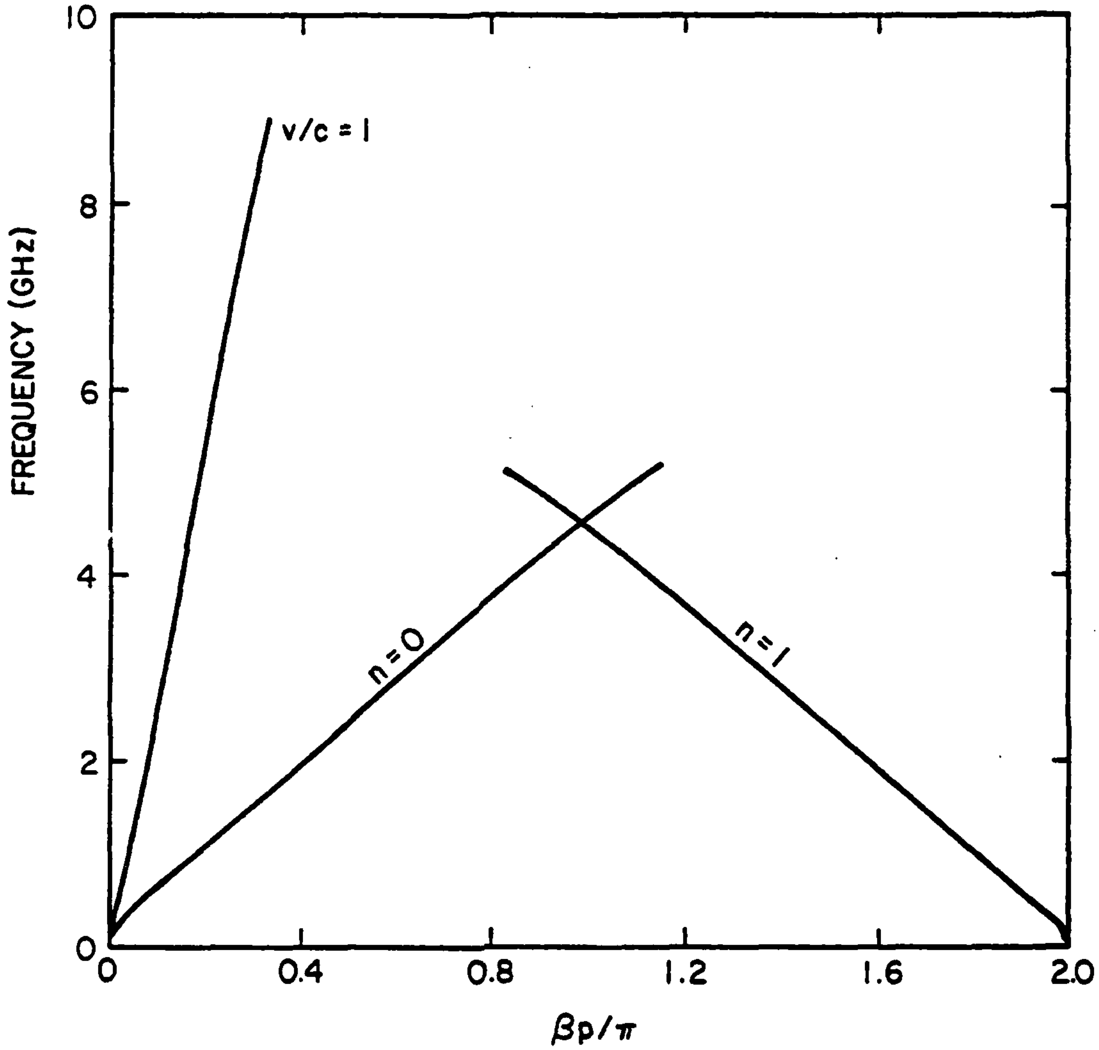


COLD TEST RESULTS FOR CIRCUIT WITH LOADING PERIOD = 5/6 PITCH

FIGURE 23

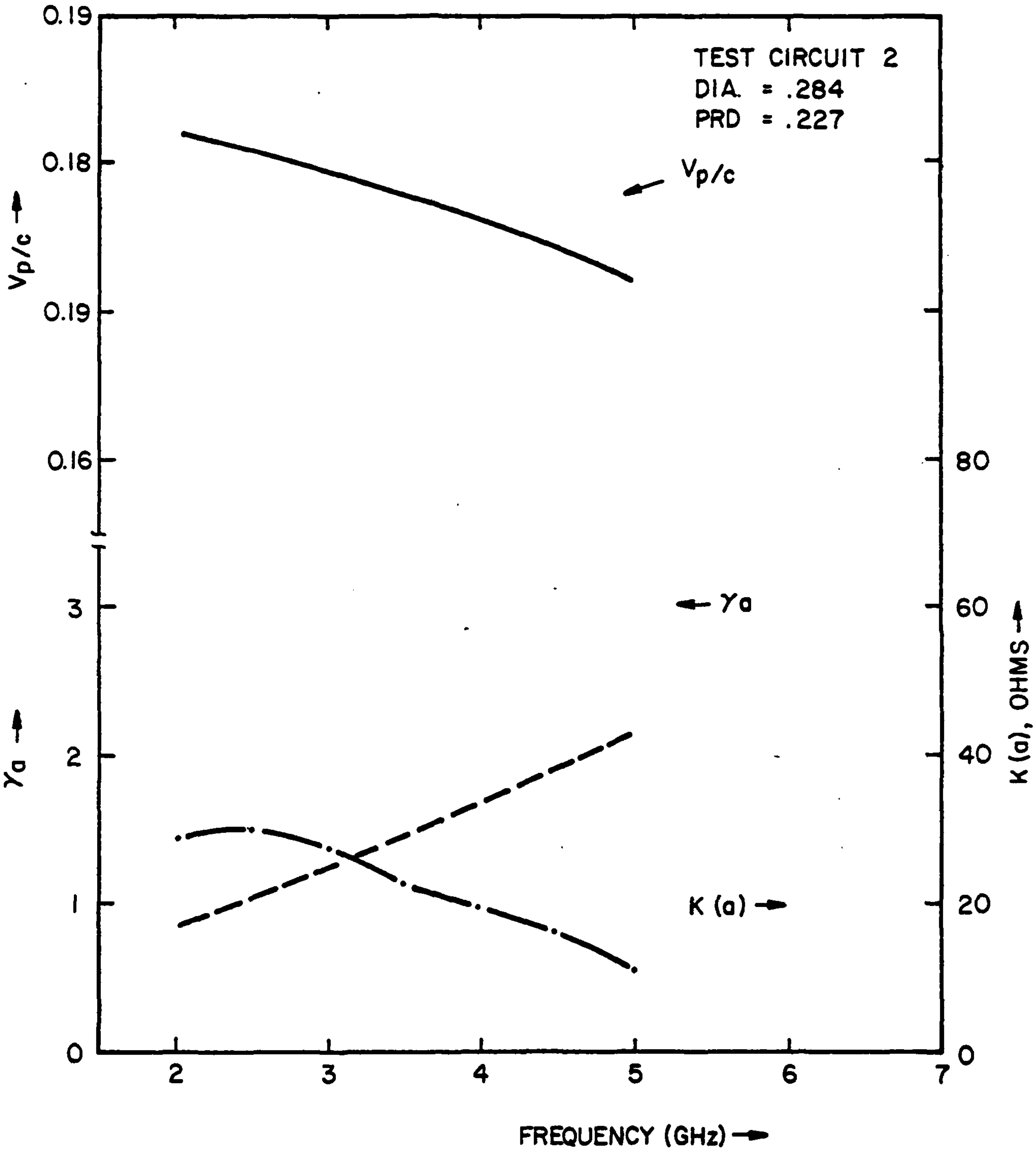


CIRCUIT IMPEDANCE FOR CIRCUIT WITH LOADING PERIOD = 5/6 PITCH

FIGURE 24

2.4 Hot Test Vehicle (continued)

lengths were modified so that the output gain was high enough to ensure high efficiency. The overall tube length was kept the same as the L-5565 so that existing package parts could be used when the tube was tested.

A summary of the tube design and its expected performance are shown in Table II.

TABLE II

EXPECTED TUBE PERFORMANCE AND DESIGN

| Performance | New 18 kV Tube L-5708-50 |
|---|---|
| Po | 10 kW |
| fo | 3.47 GHz |
| Vo | 18 kV |
| Io | 4.0 Amp |
| **Helix** | |
| $2a_s$ | 0.467 |
| $2a_m$ | 0.285 |
| pitch | 0.227 |
| tape | 0.018 x 0.110 |
| cot $\phi$ | 3.95 |

## 2.4 Hot Test Vehicle (continued)

In brazing the circuit, a sufficient degree of asymmetry was introduced by the tolerances in the parts and fixtures to "spoil" the band edge oscillation.

## 2.5 Hot Tests

One hot test vehicle was built and tested. One set of test data was teken, with helix voltages between 12 kV and 19 kV.

### 2.5.1 Low Voltage Tests

Preliminary testing was done on a test stand at which the helix voltage could not exceed 19 kV. The tube oscillated above 14 kV. Oscillation frequencies were measured from which one can derive a plot of frequency versus $\frac{\beta p}{\pi}$, as shown in Figure 25. As shown in the figure, the plot does not overlay the cold test backward wave mode. However, if the reduced velocity of the slow space charge wave, voltage depression in the beam and longitudinal electron velocity reduction due to radial and azimuthal velocity components are all taken into account, the plot of oscillations can be made to overlay the backward wave

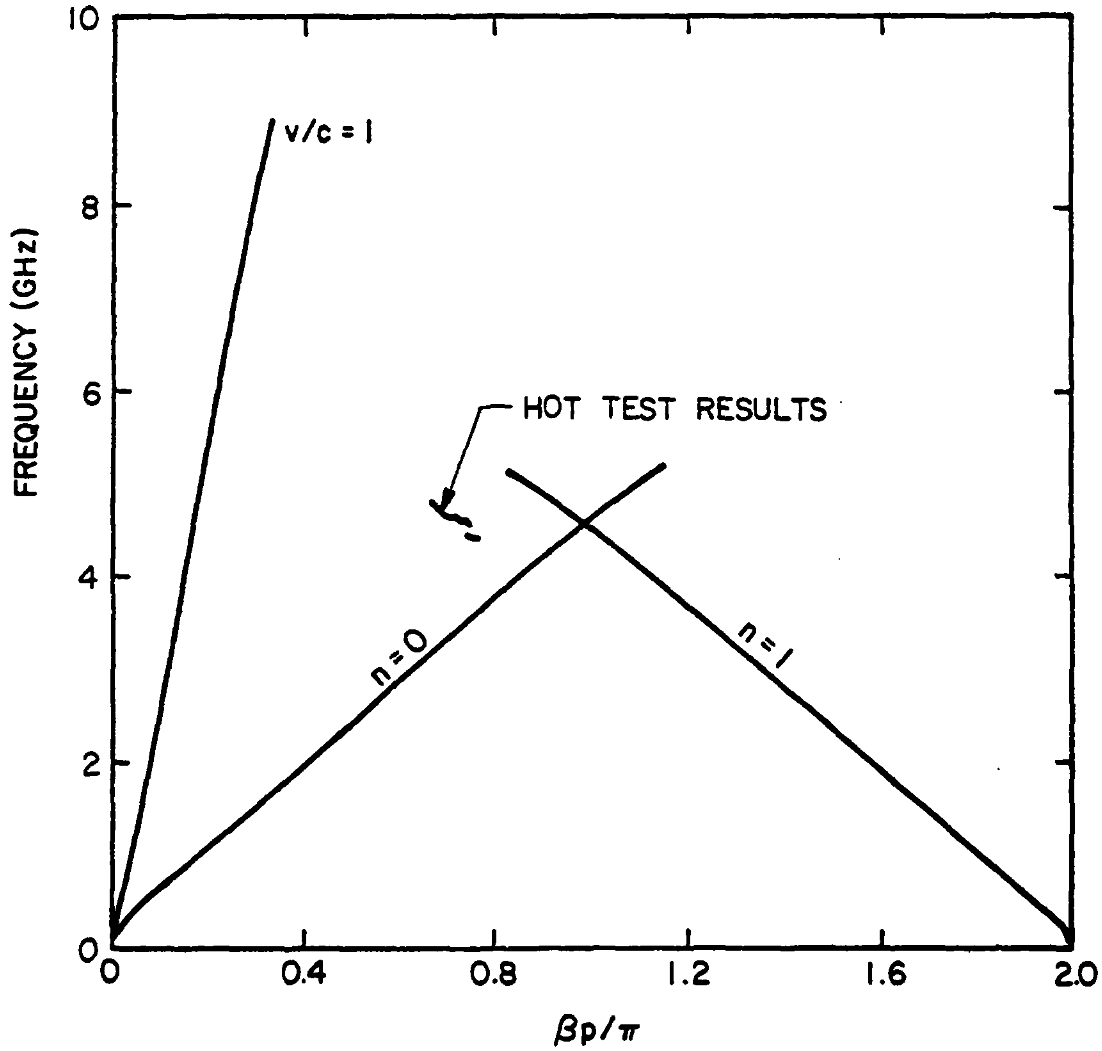


INITIAL HOT TEST DATA COMPARED TO COLD TEST DATA

FIGURE 25

2.5.1 Low Voltage Tests (continued)

mode, as shown in Figure 26. The distortions in this curve can be attributed to mode splitting at cross-over. Extrapolating from this data, the stopband should occur above 24 kV.

Start oscillation currents have also been measured at various voltages; however, there is no consistent pattern of starting current as a function of beam voltage, so this data was not plotted. Starting currents varied from 3.3A to 3.6A.

2.5.2 High Voltage Tests

If additional tests can be made, the results will be made available.

2.6 Applications at I/J Band

Because high operating voltages are possible with this type of circuit, larger helix circuits can be built for I/J band than were possible previously. In addition, helix support blocks as small as .020" on a side have been used successfully. This projects to a frequency scaling of 5.5:1, even if the voltage is held constant. If the

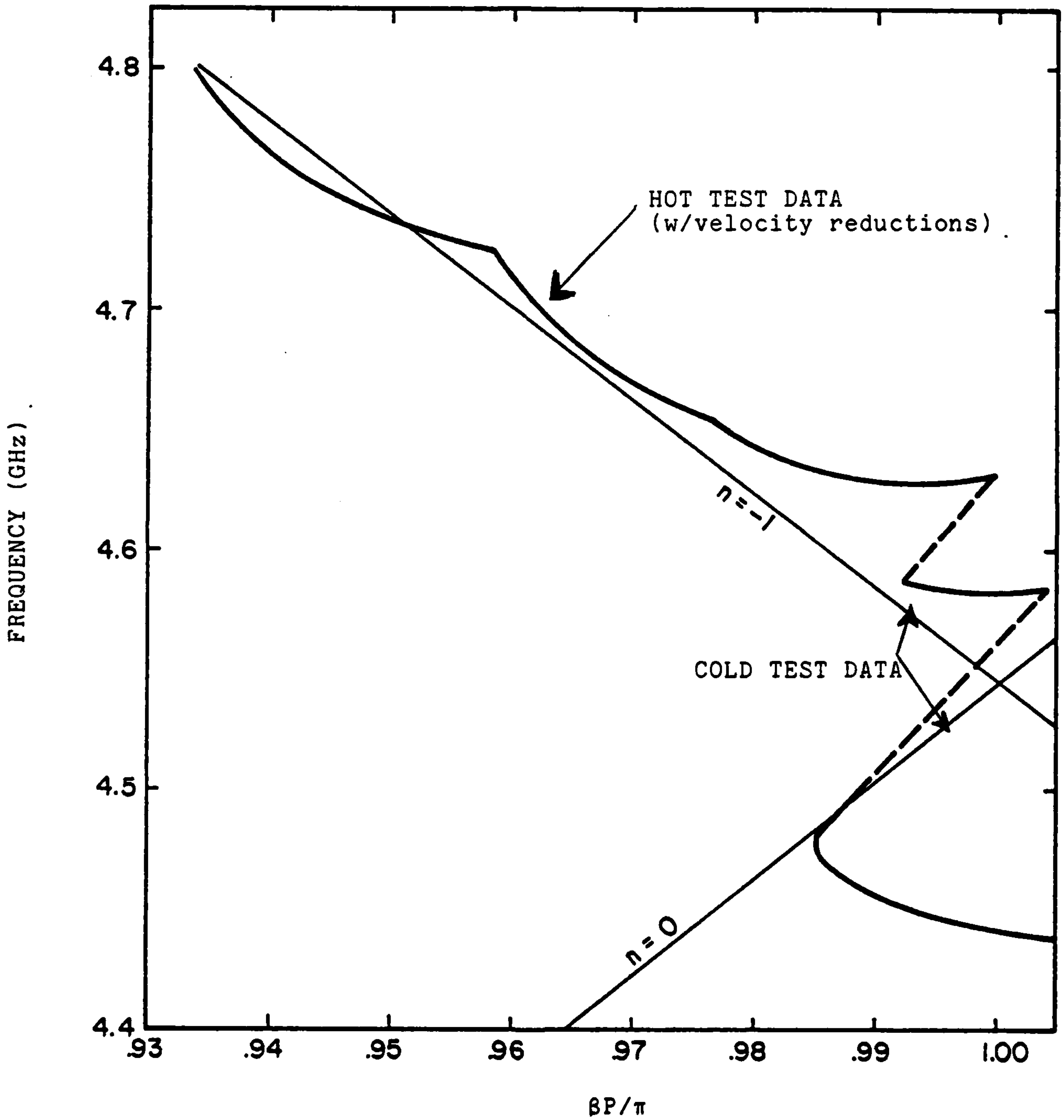


HOT TEST RESULTS ADJUSTED FOR VELOCITY REDUCTIONS

FIGURE 26

2.6 Applications at I/J Band (continued)

helix diameters used are scaled, the factor is 3.5:1. Since the operating band of the test vehicle was centered at about 3 GHz, the projected center frequencies are 16.5 GHz and 10.5 GHz respectively. A broadband I/J band tube will have a center frequency at about 13 GHz which indicates that an I/J band circuit of the type used on this program should be feasible.

## 3.0 SUMMARY AND CONCLUSIONS

An oscillation suppression technique has been proposed which has application at high voltages and high frequencies. Based on a theoretical analysis of loading in transmission lines, calculations have been made which predict the presence of stopbands. Cold tests were performed which verified the accuracy of these calculations.

A tube was built and tested. The test results indicate that the modes exist as predicted in cold test. Further testing is required to determine whether or not the stopband exists for hot test operation.

The authors wish to thank Mr. Norman Vanderplaats of NRL for his help in developing the equivalent circuit analysis.

## 4.0 PROPOSED STUDIES

Initially, work should be done to verify the existance of a stopband under hot test conditions. In addition, several potentially successful approaches to oscillation suppression can be proposed. They include:

4.1 Circuits with stopbands closer to the mode crossover point. These can be fabricated using a slight variation on the six ladder method used on this program.

4.2 Combinations of loading, pitch and helix diameter changes. Since individual blocks are used, more flexibility is possible in making circuit dimensional changes.

4.3 High frequency devices. The block supported circuit technique has already been applied to conventional I/J band tubes. Applications incorporateng oscillation suppression techniques are a natural extension of this work.

## REFERENCES


1. A.W. Lines, G.R. Nicoll and A.M. Woodward, "Some Properties of Waveguides with Periodic Structure", Proc. IEE, Vol. 97, Part III, pp. 263-276, July 1950.

2. W.J. Dodds and R.W. Peter, "Filter-Helix Traveling-Wave Tube", RCA Review, Vol. 14, pp. 502-532, December 1953.

3. A.F. Harvey, "Periodic and Guiding Structures at Microwave Frequencies", Trans. IRE, Vol. MTT-8, pp. 30-60, January 1960.

4. E.L. Lien, "Stopbands Produced by Asymmetrical Support-Rod Systems in Helix Structures", IEDM Technical Digest, pp. 412-415, December 1979.

5. N. Vanderplaats, Private Communications, July 1978.

6. H.H. Skilling, <u>Electric Transmission Lines</u>, McGraw-Hill, New York, 1951, pp. 274-279.

DAT

FILM